2-1-2016

Development of vertical diffusion solar stills utilizing folded sheets technology

Amr Seleem

THE AMERICAN UNIVERSITY IN CAIRO

SCHOOL OF SCIENCE AND ENGINEERING

Development of Vertical Diffusion Solar Still Utilizing Folded Sheets Technology

BY

Amr Mohamed Seleem

B.Sc. Mechanical Power Engineering

A thesis submitted in partial fulfillment of the requirements for the degree of Master of Science in Mechanical Engineering

Under the supervision of:

Prof. Maher Younan

Professor, Department of Mechanical Engineering
The American University in Cairo

Dr. Mohamed El-Morsi

Associate Professor, Department of Mechanical Engineering
The American University in Cairo

2016

AKNOWLEDGEMENT

I always believed that it is our sole responsibility to guarantee a sustainable source of clean drinkable water for future generations.

I love to dedicate this work for my precious family: my mother, Maha, my brothers, Shady and Mohamed, and my grandfather, Moustafa, who supported me in countless ways.

I am honored for working under supervision of Prof. Maher Younan; and am sincerely grateful for his guidance and tireless support. My deepest thank you goes to Dr. Mohamed El- Morsi for his continuous moral support; I gained priceless experience and insights through working under their supervision.

I would like to thank Qatar National Research Fund for supporting this work through the Research Grant NPRP 5-161-2-053.

ABSTRACT

Fresh water shortage is now a global problem the world is facing, and solar stills address a sustainable solution towards such crisis. This study entails the importance of desalination, specifically solar distillation. Diffusion stills have been effective in water desalination. This work presents a model of the distillation process using vertical single-effect diffusion stills. In the provided models, two geometry patterns have been utilized: the flat sheets and the folded sheets. This study aims to evaluate the applicability of utilizing folded sheets on the performance of the still using wick and without wick. A semi-analytical model utilizing the flat sheet and the folded sheet have been developed to analyze the diffusion process. Furthermore, a software computer code using Engineering Equation Solver (EES) issued to solve the equations of the developed semi-analytical model. An experimental test rig has been constructed, and used for the validation of the semi-analytical model to find its best range of validity. Also, it is validated against former literature results. A good agreement is reached with feed rates of flow up to 0.0211 kg/m^2-s. Moreover, a parametric study for the still utilizing flat sheets model is carried out to assess the performance of the still; it is found that the controllable parameters are:(i) hot plate temperature; (ii) cold plate temperature;(iii) diffusion gap thickness;(iv)feed water temperature; and (v) feed rate of flow; have an impact on the still's productivity. The most dominant parameters that influence the productivity of the still are the hot plate temperature that ranges from (55-90 °C), the diffusion gap thickness in range of (5-10 mm), the feed water temperature (20-50 °C), and the feed flow rate in range of (0.00694-0.0211 kg/m^2-s). The experimental work utilizing folded-chevron pattern sheets, both with wick and wickless, have been carried out and have been compared to the flat sheets to assess still's productivity. A comparative analysis has been conducted to evaluate the productivity; it is found that the folded sheet with wick has a higher productivity among other sheets. It indicates the superiority of the wicked folded over the wickless folded and the flat sheet. The folded pattern showed a higher performance by an average increase in the condensate to feed ratio by 27 % through the operating hot plate temperature that ranges from 60 to 90°C.

KEY WORDS

Chevron pattern, fold structure, folded sheet technology, solar desalination, solar distillation, solar still, sustainable development, vertical diffusion solar still, vertical multiple-effect diffusion solar sill, vertical single-effect diffusion still.

TABLE OF CONTENTS

LIST OF TABLES

LIST OF FIGURES

NOMENCLATURE

A	Evaporating/condensing area	m^2
CF	Condensate to feed ratio	
Cp	Specific heat capacity	J/kg-K
D	Condensate rate	kg/m^2-hr
Gr_m	Mass transfer Grashof number	
Gr_{th}	Thermal Grashof number	
h'_{fg}	Modified latent heat of vaporization	kJ/kg
k_p	Thermal conductivity	W/m-K
m_e	Condensate rate	kg/m^2-s
m_{in}	Feed rate of inlet water	mg/m^2-s
M_w	Molecular weight	kg/kmol
Nu	Nusselt number	
Pd	Partial pressure of water vapor at the distillate temperature	Pa
Pe	Partial pressure of water vapor at the evaporating temperature	Pa
Pt	Total pressure	Pa
Q_1	Input heat to the saline	W/m^2
Q_B	Brine heat	W/m^2
Q_D	Distilled heat	W/m^2
Q_{in}	Input heat	W/m^2
Q_k	Conductive heat	W/m^2
Q_L	Evaporative heat	W/m^2
Q_r	Radiative heat	W/m^2
Qs	Feed water heat	W/m^2
R	Universal gas constant	J/kmol-K

Ra	Rayleigh number	
T_{amb}	Ambient temperature	°C
T_{cond}	Condensation temperature	°C
T_{Dflm}	Distillate saline film temperature	°C
T_{evap}	Evaporation temperature	°C
T_f	Feed temperature of inlet water	°C
T_{GpD}	Condensation saline film temperature	°C
T_{GpS}	Saturation saline film temperature of	°C
T_m	Mean temperature	°C
T_P	Hot plate temperature	°C
T_{P2}	Cold plate temperature	°C
T_{Sflm}	Evaporating saline film temperature	°C
Y	Mole fraction of water	
δ_{gap}	Diffusion gap thickness	m
$\delta_{s,in}$	Saline film thickness at inlet	m
$\delta_{s,out}$	Saline film thickness at outlet	m
ζ	Diffusivity coefficient	m^2/s

CHAPTER ONE

1. INTRODUCTION

1.1. The Global Crisis

Water is a nature's gift and plays a key role in the development of an economy and, the welfare of a nation. Fresh water shortage is now a global problem that the world is facing, where 40% of the total population is suffering. Fresh water represents a small portion of the total Earth's water [1]. It represents around 3 % of the water. Almost 2% of the water is frozen in ice and covered permanently with snow. Less than 1 % of fresh water is available for the total population for the need of industry, agriculture, animals and human life as shown in Figure 1-1. People misuse the available resources of fresh water in an unsustainable way; consume much water that cause irreversible damage for the environment. [1, 2, 3]

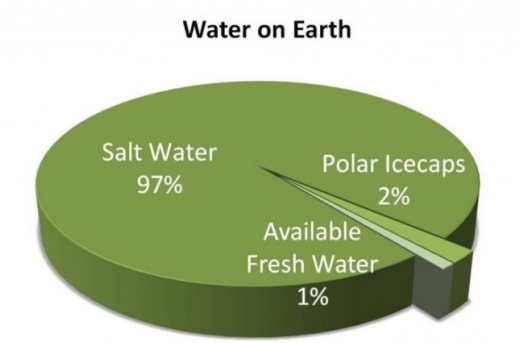

Figure 1-1: Water distribution percentage on Earth [2]

One side of the problem is the fresh water scarcity. The other face of the problem is the energy availability; the energy is now gauged as the most critical resource. The main pillar of the problem is the population growth which is rapidly increasing and the fresh water resources are limited [1]. Figure 1-2 shows the high rate of growth, in 1800, there were 800 million people that have lived. The current population is roughly 9 times of the population in 1800 which is equivalent to 6.9 billion of people, and it is estimated to grow up to 10 billion people on the planet in 2050. [4]

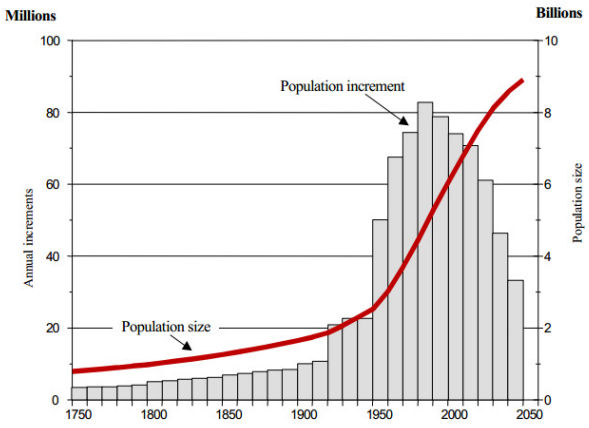

Figure 1-2: World population growth [4]

Here comes the imperative role of desalination, which is the oldest technology used by people for water purification and is considered as one of the pathways to overcome the fresh water shortage. The development in desalination technologies aim to decrease the energy consumption and minimize the environmental impacts. The new technologies have been developing to utilize renewable energy to power desalination plants. The solution to the described problematic situation should be found in consideration of the following three sustainability dimensions:

(i) Environmental dimension:

The environmental costs of desalination are not negligible and there is much debate about its extent. Basically, there are two main impacts on ecosystems that need to be addressed:

- Brine discharges and their impact on the receiving water bodies.
- Greenhouse gas emissions arising from high energy requirements.

The increase of use of desalinated water generated by renewable energy contributes to a reduction of greenhouse gases. Thus, successful development of solar stills may result in significant difference to reduce negative environmental impacts [1].

(ii) Social dimension:

Of the 6.9 billion people on earth today, 783 million people do not have access to safe drinkable water and almost 2.5 billion do not have access to adequate sanitation. Moreover, 6-8 million people die annually from the consequences of water-related diseases. This is the prime motive of the solar desalination; the social mission of the

solar distillation system is to provide safe drinkable water and also worth to mention this contributes to the urban development in coastal communities and rural areas [4].

(iii) Economic dimension:

To be able to provide a sustainable solution constantly, the proposed solution shall be economically feasible. The solar desalination can be a part of the solution to the economic growth improvement, as it helps in decreasing the gap of population growth and shortage of required energy. It supports the economy especially in the developing countries.

To achieve the economic, social and environmental objectives, the use of solar desalination represents a significant solution towards a sustainable environment; both solar energy and desalination process are combined together to provide a sustainable process to satisfy the needs of communities with fresh water in an economical and an environmental way. There are many terms that define the way of how to obtain fresh water which is safe to drink, such as water purification, water desalination, water filtration, water treatment, and water distillation.

1.2. Water Purification

Water purification is a general definition to obtain clean drinkable water that includes purification of any water sources such as seawater, surface water, ground water…etc. However, water desalination is a subcategory of water purification. Desalination is defined as water purification process to obtain drinkable water from only seawater source, it is to remove salt from seawater which is the most significant step of the process. There are several techniques of desalination that can be utilized to remove the saline from water. [5]

The most effective technique of water purification is distillation; distillation is a subcategory of water purification where it is a process of heating up any source of water (seawater, brackish water, even sewage) to make the water vaporize. The evaporated water will separate from the brackish and leaves all suspended particles, impurities, and salt condensed water becomes purified drinkable water. The Figure 1-3below shows the distribution of feed-water used in desalination plants; the most common feed-water is seawater. [6]

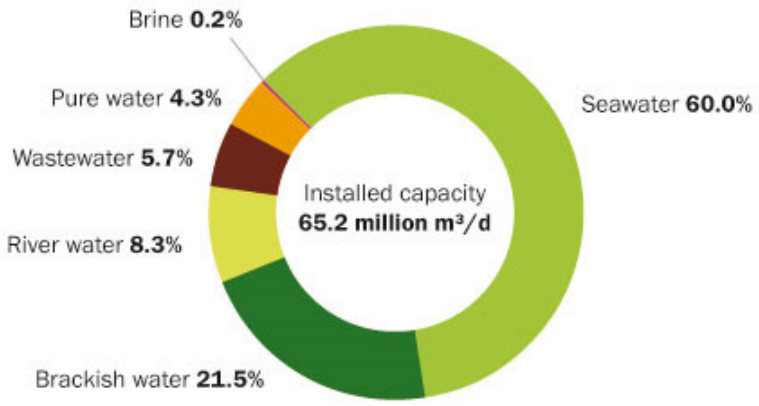

Figure 1-3: Total worldwide installed capacity by source of water [6]

Desalination

Desalination processes are classified into two main categories: Phase-change thermal separation, and membrane separation. In addition, there are other technologies such as, electro-dialysis (ED), freezing desalination and geothermal desalination. The thermal desalination is classified into multi-stage flash (MSF), multiple effect distillation (MED), and as vapor compression (VC) desalination. The distribution of the desalination technologies is presented below in Figure 1-4

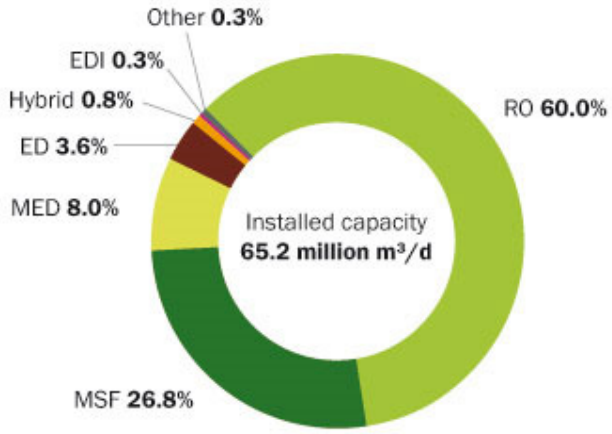

Figure 1-4: Total worldwide installed capacity by technology [6]

Distillation

Distillation requires a large amount of energy compared to the amount of produced purified water. In this technique, the water is simply evaporated using thermal energy and the resulting steam is collected and condensed as a final product. It is wonderful when a free energy is utilized; one of the modest technique is the solar still which is a very simple way to produce distilled water that is valid for drinking. [5]

All other conventional desalination technologies such as Multi-stage Flash (MSF), Multi-Effect Distillation (MED), Vapor Compression (VC), Reverse Osmosis (RO), and electro dialysis are costly and expensive for the production of small amounts of fresh water, and also have a negative impact on the environment. Solar distillation represents very attractive, economical and simple technique among other distillation processes. It is especially suited to small scale units at locations where solar energy is accessible. It minimizes the initial cost, it uses an available energy source, has low maintenance, and does not require skilled labors. The factors to be considered for the selection of solar still are: the availability of solar radiation, salt water available, cost of the still, operating easiness, maintenance cost. [5]

1.3. Solar Still

Solar distillation systems are classified into two different operation methods that are active and passive. In the active mode, an extra thermal energy by external mode is supplied into the solar still to accelerate the evaporation. The extra supplied energy could be collector, heater, or waste energy. If there is no extra supplied energy, the solar still is classified as a passive still. Active solar distillation is proven to be highly effective in cleaning up water supplies to families to provide safe drinking water. Solar distillation removes all salts and biological contaminants and microbial contamination [5, 7, 8]

Basin Solar Still

Basin solar distillation units can have many configurations, but the most conventional common is referred to as a greenhouse still. In this unit the saline water is supplied continuously to a pool of water inside the still glass enclosure, similar to a greenhouse. The black pool bottom absorbs the solar energy and heats the water. The separation process occurs between the vapor where it goes up from the brine and condenses on the cooler inside surface of the glass. The droplets of water vapor go down over the glass to be collected into small tanks as a fresh and safe water to drink. About half of the supplied water to the still was evaporated, the remained brackish water would be discarded and start the process again with saline water to be supplied into still. Figure 1-5shows the idea of simple single slope basin still. [5, 7]

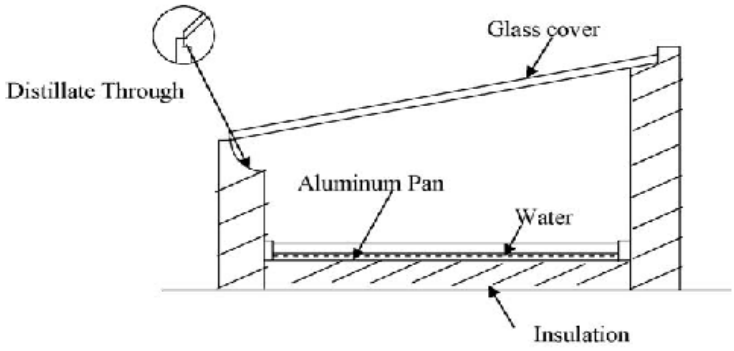

Figure 1-5: Schematic diagram of simple basin solar still [7]

Active Solar Still

The active solar stills are classified into two types: a solar still coupled with flat plate collector is working as high temperature distillation method. The solar still coupled with flat plate collector (FPC) works either in forced circulation mode or natural circulation mode. In forced circulation mode as shown in (b)

Figure 1-6 (a), a pump is used for supplying water. In natural circulation mode as shown in (b)

Figure 1-6 (b), water flows due to the difference in the density of water. The temperature of water decreases with an increase in basin area due to the large storage capacity of the water amount in the basin and depth of water. The yield increases with increase of the number of collectors. [5]

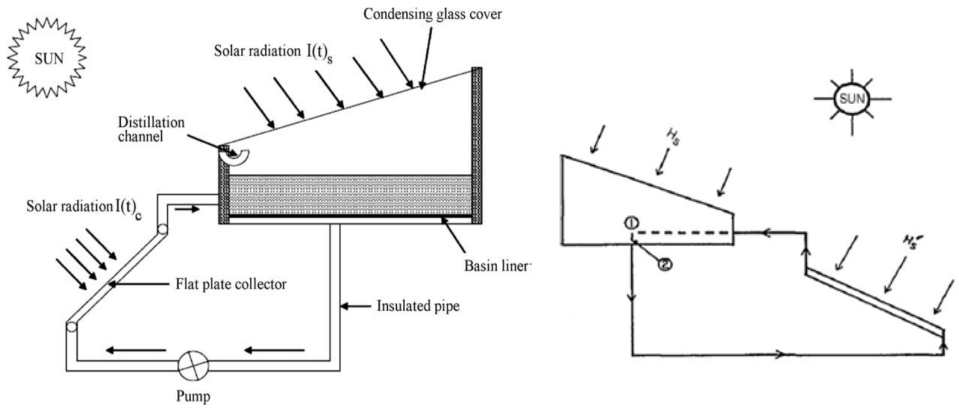

(a) (b)

Figure 1-6: Schematic solar still with (a) forced circulation mode, (b) natural circulation mode [5]

Single-Effect Diffusion Solar Still

In another type of stills which is the simple diffusion desalination still, the hot and cold surfaces are placed parallel to each other and separated by a small distance. A gas such as air fills the gap between the two surfaces. The gap thickness is selected to be small in order to suppress heat transfer by convection between the two surfaces. Solar radiation transmits through the glass cover and is absorbed on the front surface of the partition. When feed water is allowed to flow over the hot surface, water vapor diffuses across the gap where it is condensed on the cold surface. This process is called diffusion desalination. A schematic diagram of a single effect diffusion type solar still is shown in Figure 1-7 [8]

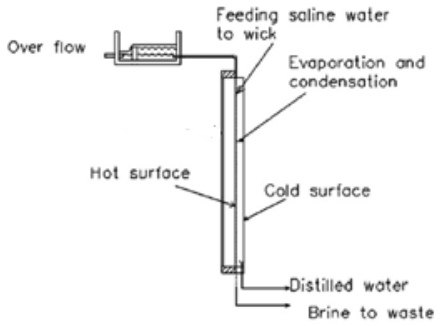

Figure 1-7: Schematic diagram of single stage diffusion still [8]

Vertical Multiple-Effect Diffusion Coupled With Basin Solar Still

There are many different types of solar stills and many configurations have been made to enhance the productivity. In multiple-effect coupled still, the basin still is coupled with the diffusion still to increase the productivity of the still as shown in Figure 1-8. It has a basin still with a triangular cross-section consisting of a sloping double glass cover facing the sun, a horizontal basin liner and a number of vertical partitions in contact with saline-soaked wicks. The vertical partitions may have small deformations, but any fibers protruding from the wicks absorb saline water, become heavier and are gradually suppressed by gravity. This makes it possible to reduce the gaps between partitions to10mm or less, which increases productivity significantly. [9, 10]

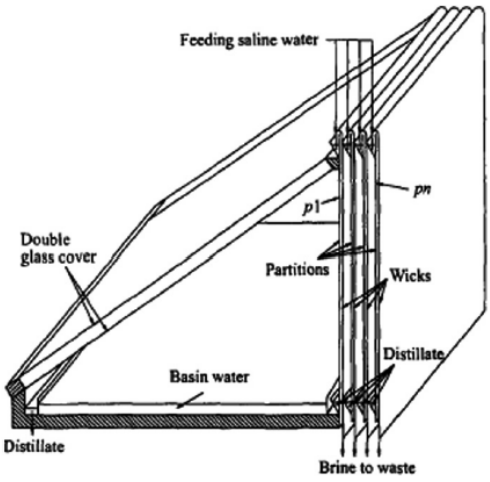

Figure 1-8: Schematic diagram of multi effect coupled solar basin still [9]

Vertical Multiple-Effect Diffusion Coupled With Collector Solar Still

One of the stills that have a high potential because of its high productivity, is multiple effect diffusion solar still. It has a great potential because of its high productivity and simplicity. Multiple effect diffusion type solar still consists of a flat plate reflector, and a glass cover and a number of vertical parallel plates with very narrow gaps between plates. [11, 12]

The saline water is fed to the wicks constantly. A schematic diagram is shown in Figure 1-9. The water vapor diffused through a humid air layer between the vertical plates and condensed on the front surface of the next plate. Latent heat from condensation is recovered to cause evaporation for the second stage. In this manner evaporation and condensation process is repeated on all stages in diffusion type still to increase the productivity of distillate. [12]

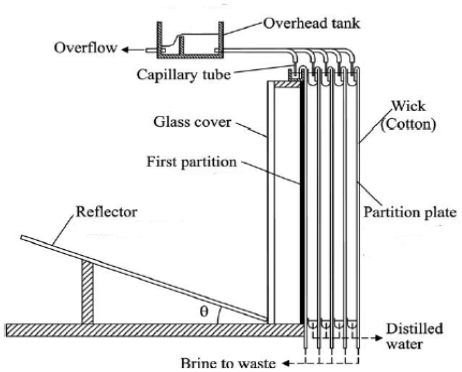

Figure 1-9: Vertical Multiple-effect diffusion solar still, coupled with a flat reflector [12]

To increase the productivity of such distillation system, the geometry of the flat vertical plates utilized in the MEDS can be modified to achieve higher productivity in the distilled yield of water.

1.4. Folded Sheets Technology

There is a new and innovative technology of sheet folding that is developed by Rutgers University [13], where these patterned (folded) sheets can replace the flat sheets with the wick traditionally that was utilized in the previous researches as shown in Figure 1-10. Folded sheets have the effect of increasing the surface area of the sheet in contact with the water for the same projected area and also induce turbulence. This will result in a subsequent increase in the efficiency of the solar still and enhance its productivity.

The new technology for sheet folding has been proven to be valuable in many applications, and resulted in three patents [13, 14]. The geometry describes folding configurations for paper, aluminum, copper, steel, other metals, composites and any other pliable sheet materials. The pattern in Figure 1-10can be folded from stainless steel, copper, or aluminum sheets and then laminated between faces to provide an efficient and lightweight ductwork of a high heat transfer rate.

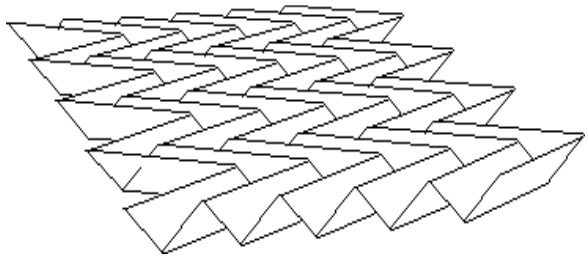

Figure 1-10: Sheet folding structure of Chevron pattern [14]

Figure 1-11 shows a machine for continuous production of folded patterns from different sheet material that was designed and built by the investigators [14]. The machine successfully folds patterns of different geometry continuously from flat sheet material with different thickness and material properties.

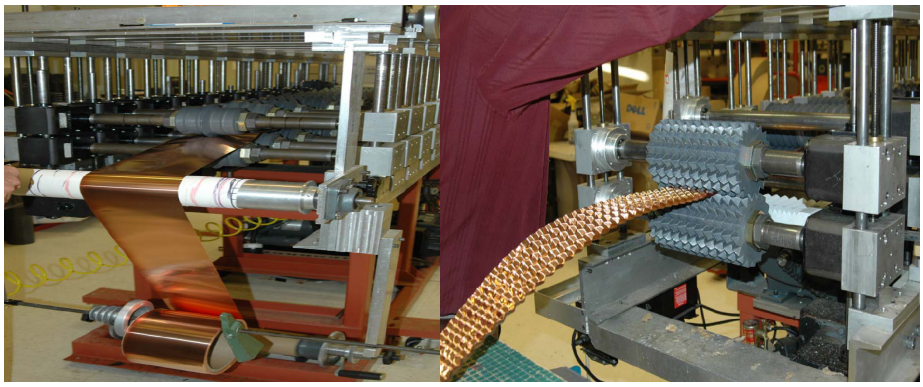

Figure 1-11: Production of Chevron folded structure by continuous folding machine from a roll stock of copper sheet material [14].

The productivity of solar driven diffusion still may be changed by the impact of utilizing new geometric patterns, based on the technology of sheet folding, in the design of single effect diffusion stills. In the following chapters (3, 4, and 5), the folded sheets technology and its application in vertical diffusion solar still will be investigated; a semi-analytical model is developed utilizing folded sheets. That model will be checked against the experimental work of folded sheets in order to find out the productivity. In addition to a comparative study between folded sheets and flat sheets.

CHAPTER TWO

2. LITERATURE REVIEW

In this chapter, a review of the previous work of the vertical single and multiple-effect of solar stills is presented; the literature presents the experimental and theoretical models of former authors. The vertical diffusion solar stills can be outlined into two streams:

2.1. Vertical Multiple-Effect Diffusion Solar Still

In Vertical Multiple-Effect Diffusion (VMED) stills, vertical parallel plates are contained within an enclosure, forming a series of partitions. Figure 2-1 shows a schematic for a two-stage diffusion still. The first plate (hot-plate) is heated, while the last plate (cold-plate) is cooled by cold saline water. Heat is supplied to heat up the hot-plate.

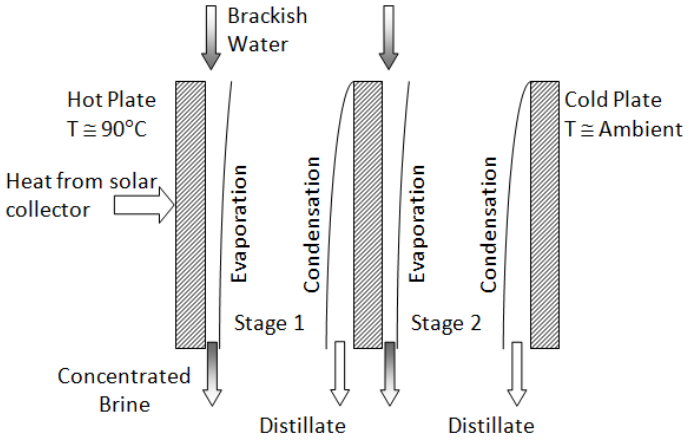

Figure 2-1: A schematic diagram of two stages of Vertical Multiple-Effect Diffusion still

The heat delivered to the hot-plate causes the saline water, fed to the first partition, to evaporate and the vapor diffuses across the gap between the two plates and condenses on the surface of successive partition. The latent heat is generated, due to the condensation phenomena and is transferred through the plate by conduction. The latent heat of condensation of the first stage is used to heat the brackish water of the second stage.

Dunkle [15]was one of the earliest who studied VMEDs. He studied experimentally the performance of a five–effect multiple-effect diffusion still. His experimental work encountered some problems. Cooper and Appleyard [16]simplified the MED system by combining the solar collector and the diffusion still into one unit. Selcuk [17] performed indoor tests for a Multiple-effect, tilted solar still to study the performance of the still. Elsayed et al [18] studied theoretically and experimentally three-effect multiple effect diffusion still. He verified the calculated results with the experimental results, and then Elsayed et al [19]presented a study of parametric conditions on the performance of an ideal diffusion still and also developed numerical correlations to predict the performance of the still. Grater, et al [20] investigated experimentally a multi-effect still for hybrid solar/fossil desalination. Tanaka et al [11]constructed eleven-effect vertical multiple-effect diffusion still. Tanaka et al [21] performed a parametric study and investigated the performance of the vertical multiple-effect diffusion still

Dunkle [15] was the first who experimentally studied the performance of multiple-effect diffusion still, five-effect still, and calculated theoretically the distilled yield and compared it to the experimental yield. He constructed the test rig and conducted experiments to investigate the effect of temperature, pressure, and diluent gas composition on the distillate yield. In his experiments, Dunkle showed many problems such as, scaling, corrosion and problems related to maintain a uniform spacing between the partitions. As a result the test apparatus was not reliable for long periods of operation. The results showed that the distillation rate increases with decrease in plate spacing, and replacing air with hydrogen as a diffusive medium; because the combination of hydrogen water vapor helps in increasing the rate of diffusion. There is a difference between predicted productivity and related it due to inaccurate temperature measurements and lack of uniform spacing between partitions. [15]

Also, Cooper and Appleyard [16]studied the multiple effect diffusion solar still. They constructed a three-effect-type still, with solar absorber plate, a glass cover parallel to the first plate. All parallel gaps of plates were covered with wicks. The plates were in contact with bottom surface effect still and utilized saline-soaked wick and the still was inclined to the sun direction. The radiation is transmitted through the glass cover and heats the first plate to cause evaporation from the plate. The constructed rig showed that it is more productive than the conventional type, such as basin-type still.

Selcuk [17] developed experimentally and theoretically a multiple-effect, tilted solar still to test its operating characteristics and determination of thermodynamic properties. He performed indoor tests for the solar sill; the water is heated artificially, using an electric heater. Instrumentation was provided for measuring temperatures, electrical heating input and distillation rates. The conducted experiments indicated that the distillate rate increases with the temperature difference between evaporation temperature and condensation temperature ($T_{evap} - T_{cond}$). He also compared the roof type solar still with multiple-effect (two effect). It is found that total distilled water of two stills is higher by 17 %. The evaporative temperature for first stage was 82 ^{0}C and condensate temperature is 64 ^{0}C. All the temperature of partitions is a function of heat supplied to the still [17]

El Sayed et al [18] studied experimentally a three-effect MEDS as shown in Figure 1-1. They also studied parameters which affect the performance of the multiple effect diffusion still. The results showed that the productivity increases with the increase in the solar radiation or the supplied heat to the still, and its reduction of the diffusion gap thickness, as well as with an increase in the number of partitions or stages. The productivity increased when the feed rate to each of the partitions was reduced. That allowed more time to evaporate the feeding saline water. The productivity increased when using helium instead of air as diluent gas; because the combination of helium water vapor helps in increasing the rate of diffusion.

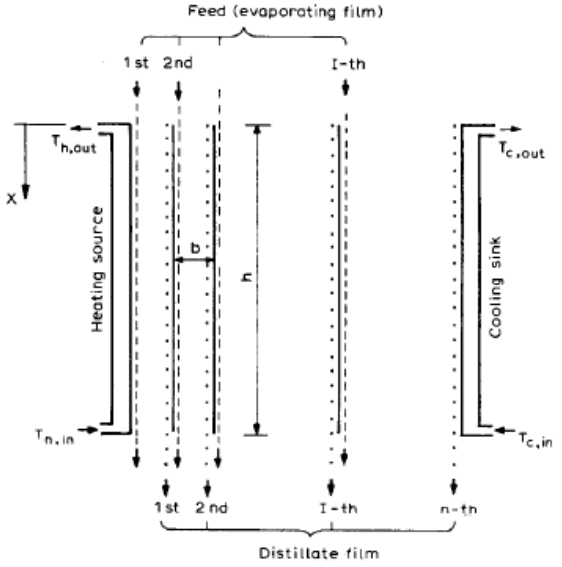

Figure 2-2: A schematic diagram of a number of multiple-effect diffusion-type still, [18]

The results produced several empirical relations to predict the average temperature of evaporative plate and the rate of distillate produced by each effect, and the productivity of the still. They found that increasing the feed, reduces the performance ratio. Increasing the heating fluid temperature or decreasing the cold fluid temperature increases the productivity and performance ratio. The model was further used to predict the performance of ten–effect diffusion still for different parametric conditions [18].

Grater et al [20] investigated experimentally a multi-effect still for hybrid solar/fossil desalination; there were different four-operation modes that have been experimentally investigated in the still. Figure 2-3shows a schematic diagram illustrating the cycle. They developed a theoretical model, and the results indicated that the distillate output increased with heating inlet temperature and increased with the decrease of cooling inlet temperature as well as the forced convection increases the distillate output at low temperatures [20].

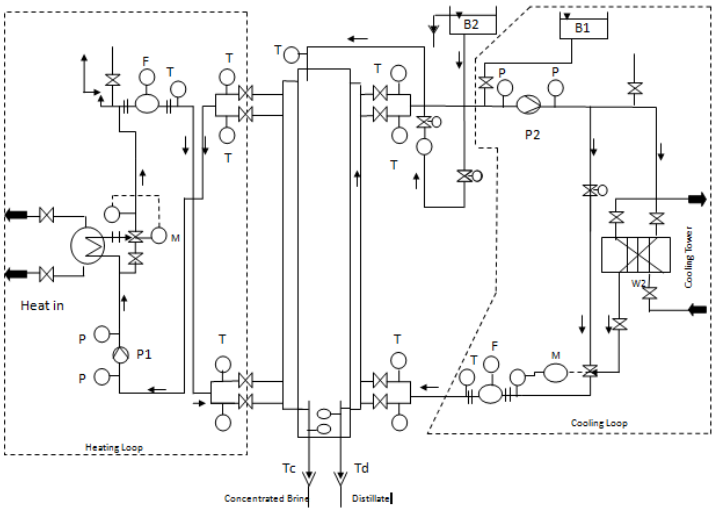

Figure 2-3: A schematic diagram of multiple-four-effect diffusion for hybrid solar/fuel still [20]

Tanaka et al [21, 22] constructed eleven-effect vertical multiple-effect diffusion still as shown in Figure 2-4 that had 5 mm diffusion gaps and produced14.8–18.7 kg/day distillate per unit effective area of the glass cover at ambient air temperature of 19–30°C. They observed that narrowing the diffusion gaps from 10 to 5 mm increased the productivity of the still. However, the productivity with 5 mm gaps was smaller than predictions by approximately 40%. The deviation from predictions was attributed

to the contact between the saline–soaked wicks and the condensing surfaces. This reduced the distillate output, without contaminating the distillate with saline water.

Tanaka et al [21, 22] performed a parametric study and investigations for the vertical multiple-effect diffusion-type solar still, which consisted of 11 numbers of partitions and diffusion gap was5 mm. The temperature of feeding saline water to wicked partitions was ambient temperature. It was found that the productivity increases with an increase in the number of partitions and the temperature of the saline water fed to the partitions. The productivity decreased with the decrease in the diffusion gaps between partitions and decrease of the feeding rate of saline water to the wicked partitions. The major impact of the productivity that enhanced the heat transfer was to lower the gap between the partitions and increase the temperature of feeding saline water. Tanaka el al showed that the productivity was about 10% larger for stills that the feeding temperature was higher than ambient temperature by 10 ^{o}C [11, 22, 21].

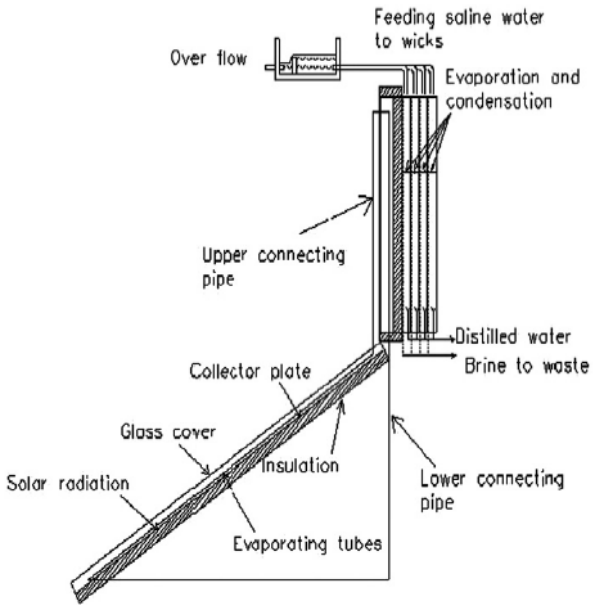

Figure 2-4: A schematic diagram of VMED, coupled with a heat pipe solar collector [21]

2.2. Vertical Single-Effect Diffusion Solar Still

This classification is simple to have a close insight to diffusion solar still. It is to investigate the evaporation and condensation processes inside the still, and to determine the heat and mass transfer within the diffusion gap. The single diffusion still is illustrated as shown above in Figure 1-7.

There are some researchers who investigated the single-effect diffusion still. Bouchekima et al [23] presented a theoretical analysis of heat and mass transfer inside a solar distiller and compared it with the experimental measurements of the distiller performance. They listed different heat and mass transfer correlations to be employed in their analytical model, and found that Somers [24] was the closest correlation to the experimental work. Nosoko et al [25] studied numerically two-dimensional heat and mass transfer in still, the transfer in both direction of saline water flowing along the plates and the direction perpendicular to the plate.

El Sayed [19] worked on the mass transfer in the diffusion gap between a vertical falling film over a heated plate and a condensing film over a parallel cooled plate in a diffusion gap. The analytical solution was based on the assumptions that the problem is steady, laminar and two dimensional (*x* and *y*). The evaporating falling film was assumed to have constant thickness i.e. mass diffused was small with respect to the mass flow rate of the film.

$$\dot{m_e} = \frac{\zeta * M_w}{RT_m} \frac{P_t}{\delta_{gap}} \ln \frac{P_t - P_c}{P_t - P_e}$$

Where:

The evaporation heat transfer coefficient was defined as follows:

$$h_e = m_{evap} h_{fg} / (T_{evap} - T_{cond})$$

Using helium instead of air, the heat transfer coefficient was more than doubled. However, the increase of diffusion and condensation increases the thickness and the thermal resistance of the condensation layer and evaporating layer which decreases heat transferred to the 2nd plate.

Fathalah et al [26]also derived empirical correlations for condensate rate D which is in Kg/m^2hr, and the evaporative heat transfer coefficient h_e which is in W/m^2K and both are function in the evaporation temperature Te which is in ^oC. The correlations were applicable for Te ranging from 50 ^0C to 90 ^0C and were also applicable for Condensing temperature Tc ranging from 20 ^0C to 40^0C, and only for air diffusive medium for 6 mm gap.

$$D = -27.28 + 1.42\,T_e - 2.53x\,10 - 2\,(T_e)^2 + 1.64 * 10 - 4(T_e)^3$$

$$h_e = 171.57 + 9.96\,T_e - 0.167\,(T_e)^2 + 1.12\,x10 - 3\,(T_e)^3$$

From the results of the computations, increasing the evaporation temperature or decreasing the diffusion gap width caused appreciable increase in the condensate rate D, and the evaporative heat transfer coefficient h_e. Also decreasing the condensation temperature slightly increased the condensate rate D, and slightly decreased the evaporative heat transfer coefficient h_e.

Fathalah et al [26]presented a numerical study of evaporation-condensation in a vertical diffusion gap and carried out a comprehensive analysis of the effect of evaporating temperature, condensing temperature, and diffusion gap width over the diffusion mass flow rate and evaporation heat transfer coefficient.

Tafreshi et al [27] derived a correlation of mass transfer from a vertical wet fabric using the obtained correlation by Churchill and Chu [28] and showed agreement with experimental trial. Raach, and Mitrovic [29] numerically studied the problem of an evaporating saline film running down a vertical flat plate maintained at constant temperature in the presence of turbulence wires immersed in the evaporating film. Raach, and Mitrovic [30] simulated an evaporating seawater film running down a vertical plate of constant temperature.

Bouchekima et al [23] developed a capillary film "Solar Distiller" of simple construction that produced $1m^3$/day of fresh water. The test-rig, shown in Figure 2-5, was very simple, and easy to maintain. They studied experimentally and theoretically this solar still and made a comparable study of correlations for calculation of heat transfer coefficients in the process of evaporation and condensation to verify it. The results showed that the distillate rate is increased with the increase of temperature of brine, and when increasing the number of plates. The results were in agreement with the theoretical equation of the correlation of Somers [24]

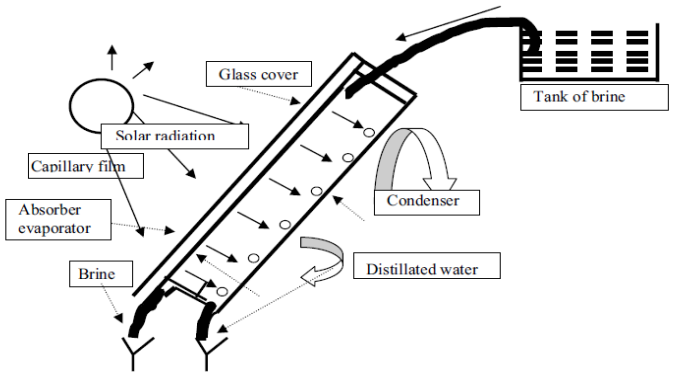

Figure 2-5: A schematic diagram of a number of multiple-effect diffusion-type still [23]

Somers [24] presented a problem that involves evaporation and condensation phenomena with free-convective thermal and mass transfer from a wetted isothermal vertical plate to a gas at ambient temperature and mass concentration different from that on the plate. In developing the control equations for a thermal mass-transfer process, Somers developed the motion equation, diffusion equation and energy equation.

$Nu_{xy}= A(C_0, T_{amb}/T_0, Sc, Pr) [Gr_x +(Pr/Sc)^{1/2} Gr_{yz}]^{1/4}$

where A is a function of concentration difference (C_0), ratio of ambient and plate temperatures (T_{amb}/T_0) and Prandtl (Pr) and Schmidt (Sc) numbers. Approximate values for A and temperature ratio's are: A = 0.38, Pr/Sc = 0.75.

He developed an approximate correlation for combined thermal and mass transfer on a vertical-flat-plate is as follows:

$Nu_{xy}= 0.38 [Gr_{th} +0.87Gr_m]^{1/4}$

This Somer's equation wasof help to calculate the convective heat transfer coefficient.

Raach and Mitrovic [29]numerically studied the problem of an evaporating saline film running down a vertical flat plate maintained at constant temperature in the presence of turbulence wires immersed in the evaporating film shown in Figure 2-6. The investigation is focused on methods to decrease the thermal resistance of the evaporating falling film. This is achieved through the use of turbulence wires immersed in the film. The system is numerically investigated. The results showed that introducing the turbulence wires increased the evaporation rate. This led to the conclusion that the heat transfer can be augmented by the use of turbulence wires.

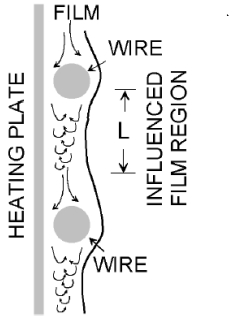

Figure 2-6: Schematic diagram of a liquid falling along a vertical plate over horizontal wires [29]

2.3. Scope of Work

The literature review shows a significant amount of research has been conducted on vertical diffusion solar stills. Part of literature is about development of numerical and experimental models and verifying them against each other. The other part is theoretically focused on the heat and mass transfer inside the diffusion gap.

In the literature, the conducted experimental work, the flat vertical plates in contact with saline-soaked evaporation wicks mainly have been utilized as an evaporation surfaces. The wicks are utilized to (i) stabilize the feed of saline water over the plate (ii) reduce the velocity of saline water to enhance the heat and mass transfer. The literature also reveals that there is no simple semi-analytical models that can predict the performance of vertical diffusion stills. The current work investigates the applicability of folded sheets for vertical diffusion solar stills. Therefore, the objectives are:

(1) Develop a semi-analytical model of a vertical single-effect diffusion solar still utilizing flat sheets with wick;

(2) Construct an experimental test rig to examine the performance of single-effect diffusion solar still utilizing flat sheets and folded-chevron pattern sheets;

(3) Validate the semi-analytical model of flat sheet against the experimental results of flat sheet, and also against experimental work of former authors

(4) Carry out a parametric study based on the semi-analytical model of flat sheet to identify the influential parameters of the productivity;

(5) Develop a semi-analytical model of a vertical single-effect diffusion solar still utilizing folded sheets without wick.

(6) Validate the semi-analytical model of folded sheets against the experimental results of folded sheets.

(7) Make a comparative study for the performance of utilizing flat sheet with and without wick against the folded chevron-pattern sheet.

CHAPTER THREE

3. METHEDOLOGY

In this chapter, analytical and experimental models are presented. A semi-analytical model is developed for single-stage diffusion still utilizing a flat sheet. The semi-analytical model is validated against the experimental work and also with other former author's work. Furthermore, a parametric study is presented in chapter 4 that is based on the semi-analytical model to investigate the performance of the still.

3.1. Semi-Analytical Model

In the literature, numerous studies on vertical diffusion stills have been carried out theoretically and experimentally to determine the productivity and investigate the operation parameters. Dunkle [15] was the first who provided a theoretical and experimental analysis for the diffusion still. The calculated and experimental results were not in good agreement due to encountered problems such as temperature measurements, and lack of uniform spacing between plates. El Sayed et al [18, 19, 26], studied experimentally the diffusion stills and provided a mathematical analysis. However, their provided mathematical models did not show details. Tanaka et al [9, 10, 21] constructed the diffusion stills for experimental testing, and then performed theoretical analysis for verification of the experimental results.

In this proposed semi-analytical model, a theoretical and thermal analysis is carried out for each stage of the diffusion still for the flat type and folded chevron pattern type. The folded type has never been studied in the literature. This study approach is to present a theoretical model on the diffusion still, and then verify the developed model by experimental work.

For accurate analysis of the performance of the single-effect diffusion still, it is better to study theoretically the two-dimensional heat and mass transfer in the still, in both the direction perpendicular to the plates and the direction of saline flowing over the plates.

In the presented semi-analytical model, shown in Figure 3-1, the model consists of two isothermal plates facing each other vertically. One of the plates is hot, and the other one is the cold plate. A saline film flows over the hot plate by the gravity force, as a

result the temperature of the film increases. The saline film evaporates and the vapor diffuses within the gap between the two plates and then condenses over the cold plate.

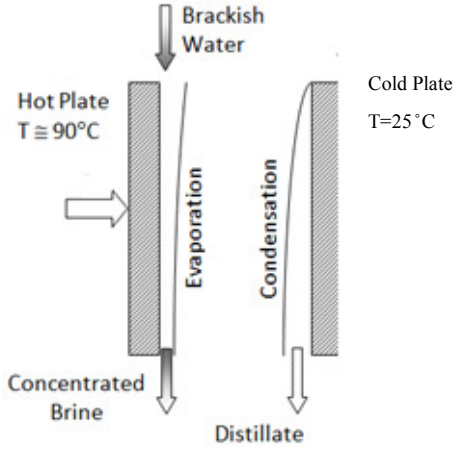

Figure 3-1: A schematic diagram of proposed single-effect diffusion still

3.1.1. Flat Sheet

The proposed semi-analytical model has been developed aiming to describe the thermal structure of the system and predict the system's yield. The developed model has been constructed using the basic equations of heat and mass transfer.

Dunkle [15] provided thermal circuit to his proposed still, but does not provide a detailed theoretical analysis to each stage of the diffusion still that matches his proposed thermal circuit [15]. Both Tanaka et al [9] and El Sayed et al [18] did not provide a detailed thermal circuit for their proposed stills. It is important to present the thermal resistance between the two plates to simplify the heat analysis of the model. The thermal circuit shown in Figure 3-2 explains the thermal energy flow through the system from the heat source to the heat sink.

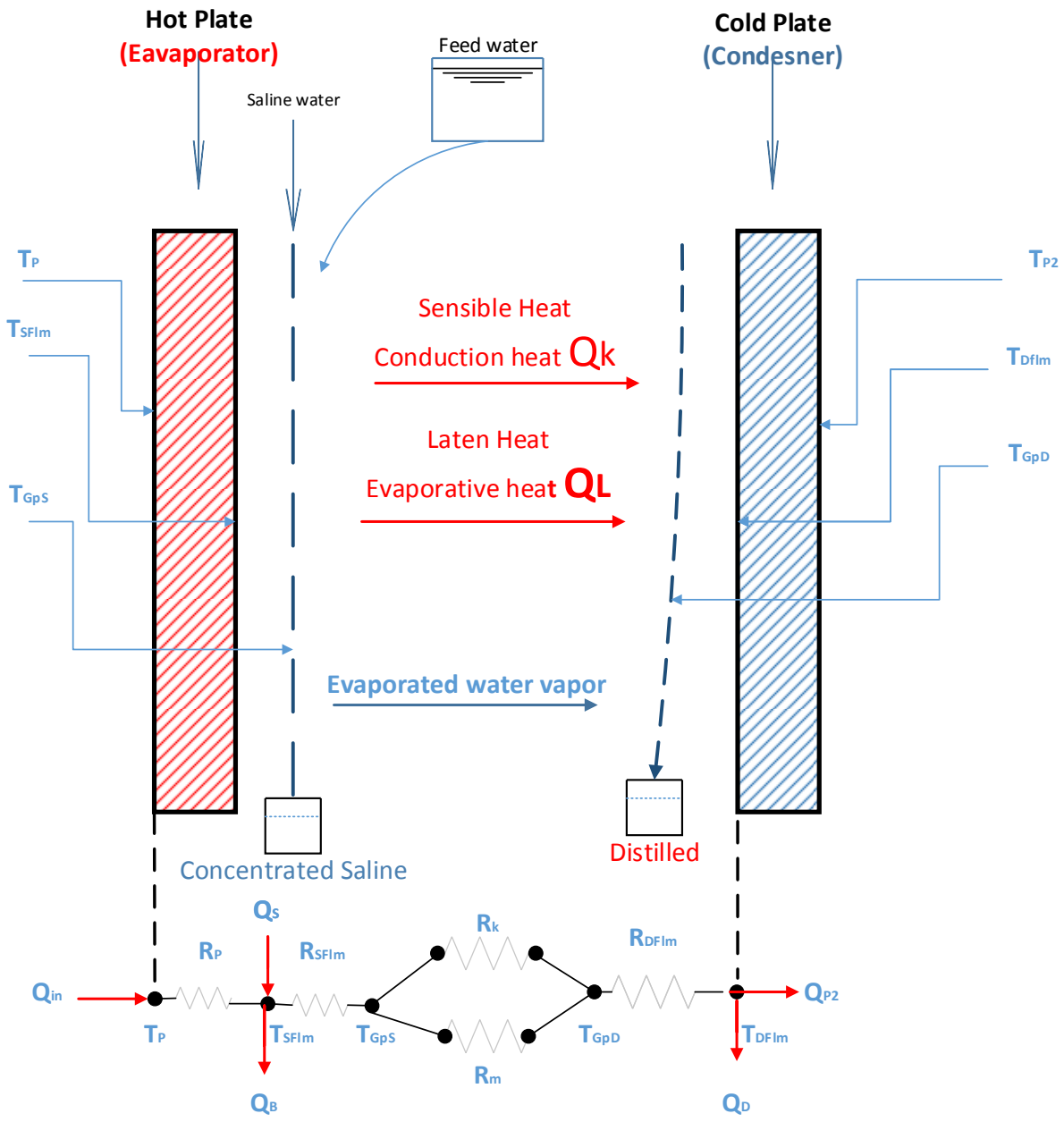

Figure 3-2: A schematic diagram of the thermal resistances for single effect diffusion still

3.1.1.1. Energy Balance

In Figure 3-2, the heat absorbed by the hot plate is coming from an Electric heater, $\dot{Q}_{in}$, is conducted through the first plate, hot–plate. Part of this energy together with the energy introduced to the partition with the incoming feed of saline water, $\dot{Q}_{s}$, is lost as

the concentrated brine leaves the partition, $\dot{Q}_B$. This energy balance is expressed by equation 1

The model is based on the following assumptions:

- The thickness of diffusion gap is so small, the heat transfer by convection is suppressed between the evaporative and condensing surface [19].
- The feed water film is maintained at constant temperature T_{swin} [19]
- The evaporation and condensation plates have the same area as the feed water film.
- The hot plate has a constant temperature T_p
- The cold plate has a constant temperature T_{p2}
- The feed, saline, distillated water have a constant and equal specific heat C_p

The following equations represent the correlations that govern the system. According to the first law of thermodynamics, the amount of heat transferred to the hot plate that is generated by the effect of electric heaters can be determined based on steady-state energy balance:

$$\dot{Q}_1 = \dot{Q}_{in} + \dot{Q}_S - \dot{Q}_B \tag{1}$$

The thermal energy $\dot{Q}_1$ flowing through the air gap of the first partitions is of two components; sensible, $\dot{Q}_S$, and latent, $\dot{Q}_L$. The sensible energy is transferred across the gap by conduction, $\dot{Q}_k$, convection, $\dot{Q}_c$, and radiation $\dot{Q}_r$. This energy balance is expressed by the following equation

$$\dot{Q}_1 = \dot{Q}_k + \dot{Q}_c + \dot{Q}_r + \dot{Q}_L \tag{2}$$

Dunkle stated that pure conduction and diffusion occurs when plates are spaced closer than 12.5 mm [15]. The convection heat transfer $\dot{Q}_c$ and the radiation heat transfer $\dot{Q}_r$ across the gap are neglected due to the small gap as it has been implemented with El Sayed model. [19]

As the vapor condenses on the subsequent plate the vapor releases latent heat of condensation. Part of the latent heat is lost as the condensate leaves the partition and

the rest is conducted through the plate to heat the saline water running on its back. The energy given to the second plate is expressed by this equation

$$\dot{Q}_2 = \dot{Q}_1 - \dot{Q}_D \quad (3)$$

Substituting by equation 1 in equation 3,

$$\dot{Q}_2 = \dot{Q}_{IN} + \dot{Q}_S - \dot{Q}_B - \dot{Q}_D \quad (4)$$

3.1.1.2. Transport equations

The following equations describe how the energy is transferred through the diffusion still through each layer; especially the middle one (the diffusion gap) that involves heat and mass transfer.

1. In the first layer, energy is transferred from the heat source through the first plate. The energy is used to heat the falling film, applying Fourier's law across the hot-plate:

$$Q_{in} = \frac{T_p - T_{Sfilm}}{R_p} \quad (5)$$

where, T_p is the temperature of the hot–plate, T_{Sfilm} is the temperature of the hot–plate from the saline–film side, as shown in Figure 3-2, and R_p is the thermal resistance of the plate defined as

$$R_p = \frac{\delta_{hp}}{A * k_p} \quad (6)$$

where, A , δ_p and k_p are the surface area, thickness and the thermal conductivity of the plate, respectively. The thermal conductivity of evaporation plate's material k_p is evaluated at average temperature ($\frac{T_p + T_{Sfilm}}{2}$).

2. In the second layer, energy is transferred from the hot plate across the falling saline film. To determine the heat transfer across the saline film, Nusselt's theory gives a parabolic velocity profile and a linear temperature distribution, as defined:

$$Q_1 = \frac{T_{Sfilm} - T_{Gps}}{R_{Sfilm}} \tag{7}$$

where, T_{GpS} is the saturation temperature of the vapor, which is assumed to be equal to the temperature of the liquid–gas interface on the saline–film side, and R_{Sfilm} is the thermal resistance of the evaporating saline film defined as:

$$R_{Sfilm} = \frac{\delta_{Sfilm}}{A * k_{Sfilm}} \tag{8}$$

where, k_{Sfilm} is the thermal conductivity of the saline that can be evaluated at an average temperature ($\frac{T_{Sfilm}+T_{Gps}}{2}$).

With the view to slow mass feed rate, the flow can be considered laminar for the liquid film and have a constant temperature along the hot plate. According to Nusselt theory, the thickness of saline film can be obtained by [32]:

$$\delta\,(x) = \left[\frac{4k_l\mu_l(T_{Sat} - T_s)x}{g\rho_l(\rho_l - \rho_v)h'_{fg}}\right]^{\frac{1}{4}} \tag{9}$$

Despite the fact of complexity associated with identifying the film thickness, it is convenient to utilize Equation. (10) that predicts the average thickness of saline film according to the Nusselt's theory by integrating equation no. 9 from$\delta_{s,in}$, to $\delta_{s,out}$ [32]:

$$\delta_{Sfilm} = \frac{4}{5L}\frac{\rho_{Sfilm}\left(\rho_{Sfilm} - \rho_g\right) * g * h'_{fg}}{4k_{Sfilm}\mu_{Sfilm}\,(T_{Sfilm} - T_{Gps})}\,({\delta_{s,in}}^5 - {\delta_{s,out}}^5) \tag{10}$$

where g is the gravitational acceleration, L is the length of saline film,ρ_{Sfilm} and $\mu_{Sfilm}$are the density, and viscosity evaluated at average temperature ($\frac{T_{Sfilm}+T_{Gps}}{2}$), respectively.$\delta_{s,in}$, and $\delta_{s,out}$ are the thickness of the saline film at the partition inlet and outlet, respectively.

In order to determine the initial film thickness, it may be defined using the empirical correlation of flow measurement of the Kindsvater-Carter rectangular weir equation [33]:

$$Q = C_e \frac{2}{3} \sqrt{2g}\,(b + k_b)(h + k_h)^{\frac{3}{2}} \tag{11}$$

Where Q is the discharge, Ce is the discharge coefficient, g is gravitational acceleration, h is the head, b is the notch width, and k_b and k_h are account for effects of viscosity and surface tension.

Equation (12) is obtained after applying the geometry of utilized feeding box in equation (11). As a result, the initial thickness of the saline feed at the upper edge of the hotplate $\delta_{s,in}$ can be evaluated using an empirical correlation deduced from the rectangular weir equation [32]:

$$\delta_{s,in} = \left(\frac{\dot{m}_{in}}{760}\right)^{\frac{2}{3}} \tag{12}$$

By substituting in equation (9), taking into consideration that thickness at, x=0, is equal to $\delta_{s,in}$, thus the thickness at outlet $\delta_{s,out}$, can be evaluated as:

$$\delta_{s,out} = (\delta_{s,in}{}^4 - L\frac{4k_{Sfilm}\mu_{Sfilm}\,(T_{Sfilm} - T_{Gps})}{\rho_{Sfilm}\left(\rho_{Sfilm} - \rho_g\right)g h'_{fg}})^{\frac{1}{4}} \tag{13}$$

where, ρ_g, is the density of the vapor phase evaluated at saturation temperature T_{GpS}. $\rho_{Sfilm}$and $\mu_{Sfilm}$are the density and the viscosity of the evaporating saline film, respectively, evaluated at the average temperature $\bar{T}$= ($\frac{T_{Sfilm}+T_{Gps}}{2}$).

As Rohsenow [32] recommended using a modified latent heat of vaporization,h'_{fg}that can obtained by:

$$h'_{fg} = h_{fg} + 0.68\,C_p(T_{Sfilm} - T_{Gps}) \tag{14}$$

Where C_p is the specific heat of evaporating saline film estimated at the average temperature $\bar{T}$= ($\frac{T_{Sfilm}+T_{Gps}}{2}$).

3. In the third layer, the energy is transferred from the saline film to the diffusion gap. It is pretty similar to what has been done in literature with Dunkle [15] and El Sayed et al [18]. It includes the transfer of sensible and latent heat phases; the sensible heat is assumed to be conduction with the view to slow rate of saline film. The latent heat is transferred to the condensing side through mass diffusion. The conduction heat transfer across the air gap is simply obtained by applying Fourier's law:

$$Q_k = \frac{T_{GpS} - T_{GpD}}{R_k} \tag{15}$$

where R_k is the conduction thermal resistance of air in the gap expressed as:

$$R_k = \frac{\delta_{Gp}}{A * k_{Gp}} \tag{16}$$

where δ_{Gp} and k_{Gp} are the thickness and the thermal conductivity of the trapped air in the gap

The latent component is estimated using the following equation:

$$\dot{Q}_L = \dot{m}_{evap} * h_{fg,Gps} \tag{17}$$

$\dot{m}_{evap}$ is the amount of evaporated water from the falling saline film and diffused through the air gap and finally condenses on the subsequent plate. h_{fg} is the latent heat at T_{GpS}. The diffusion equation through a stationary gas is used to calculate the mass transfer across the gap as following equation [18, 15]

$$\dot{m}_{evap} = \frac{\zeta M_w * 10^3}{\bar{R}(\bar{T}_i + 273)} \frac{P_T}{\delta_{\mathrm{Gp}}} ln \frac{P_t - P_{di}}{P_t - P_{ei}} \tag{18}$$

Where P_{di}, and P_{ei} are partial pressures in the diffusion gap, and ζ is the diffusion coefficient that can be expressed using the following equation [18]:

$$\zeta = 0.911 * \frac{10^{-6}}{P_T}[\frac{(\overline{T_l} + 273)^{2.5}}{\overline{T_l} + 518}] \quad (19)$$

$$where, \overline{T_l} = \frac{T_{hp} + T_{cp}}{2} \quad (20)$$

where M_w is the molecular weight of water-vapor, and P_T is the total pressure (kPa), and T_{cp} is the cold plate temperature.

3.1.2. Folded Sheets

Some modifications have been carried out on the semi-analytical model to describe the thermal performance of the folded type vertical diffusion still. The case of folded sheet contains complications to present semi-analytical model. It has not been done before in the literature.

The expected difference in the description of the folded type from the flat type is concentrated in the heat transfer process from the hot plate to the saline film. The heat transfer is function of heat transfer coefficient and the surface area. The chevron pattern enhances the surface area, which in return increases the efficiency of heat transfer across the plates. At high rates of feed flow, turbulence due to the folding should be considered as it raises the heat transfer coefficient.

The proposed method is converting the identification of the working length of the folded plate into the identification of the effective length of the path that the saline takes down over the plate.

Applying the concept of the effective length using the following equation:

$$L_{eff} = \frac{L}{Sin\,(\theta)} \tag{21}$$

Where L_{eff} represents the effective path that the saline flow is supposed to take, L is the original sheet length, and θ is half the angle between two sides as shown in Figure 3-3 and Figure 3-4: A building block of Chevron pattern sheet.

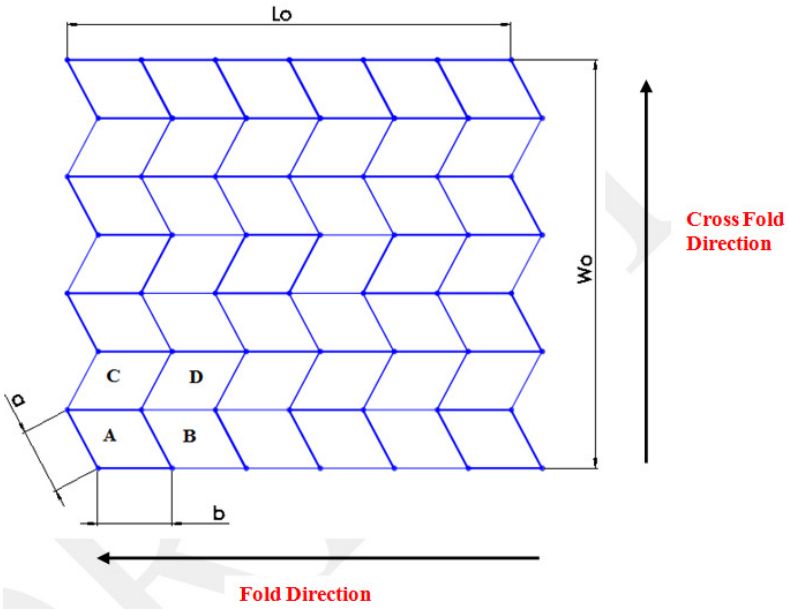

Figure 3-3: Top view of the chevron pattern in use [35]

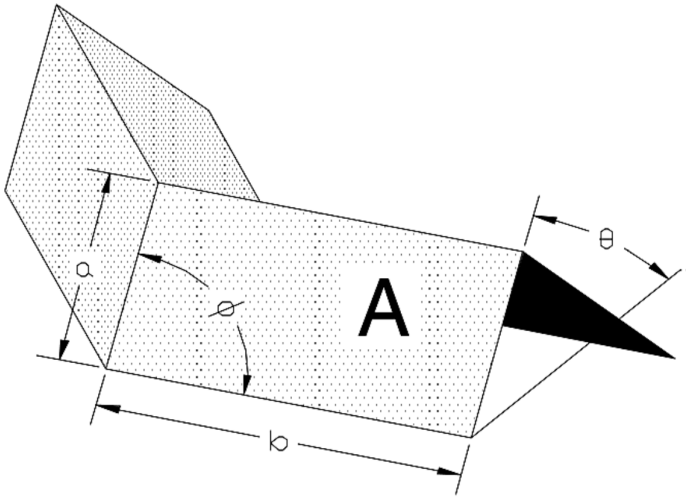

Figure 3-4: A building block of Chevron pattern sheet [35]

The geometry of folded chevron-pattern sheet can be defined as:

a Length of the parallelogram, (m)

b Width of the parallelogram, (m)

φ Parallelogram angle, (degrees)

θ Folding angle (degrees)

3.1.3. The Analytical Code

A simple analytical code is developed to predict the performance of a single-stage diffusion still and invalidated against former authors. The mathematical model is built by Engineering Equation Solver (EES) to run on the model to result in a parametric study to show the influence of parameters on the performance of the still.

The dominant parameters that enhance the performance of the still and influence the performance ratio are the following:

- The mass flow rate of feed water m_f
- Hot plate temperature T_p
- Diffusion gap δ_{gap}
- Cold plate temperature T_{p2}
- Ambient Temperature T_{amb}

In the following chapter 4, the results of the developed analytical code shows the relation between the parameters and the productivity of the still.

3.1.3.1.The Analytical Code Input

- feed flow rate of saline water $\dot{m}_{s,in}$, kg/m^2-s
- Hot plate temperature T_p, C
- Cold plate temperature T_{p2}, C
- Ambient temperature T_a, C
- Feed water temperature $T_{sw,in}$, C
- Evaporation/condensation surface area, m^2
- Length of hot/cold plate L, m
- Diffusion gap, δ_{GP}mm
- Plate thickness δ_p

3.1.3.2.The Analytical Code Output and Performance Calculations

- Condensate, (m_{evap})
- Condensate to Feed Ratio, (CF)
- Evaporative Heat (Heat to the cold plate), (Q_{evap})
- Evaporative and mass heat transfer coefficient, (h_m)

The following flow chart Figure 3-5 describes the structure of the analytical code.

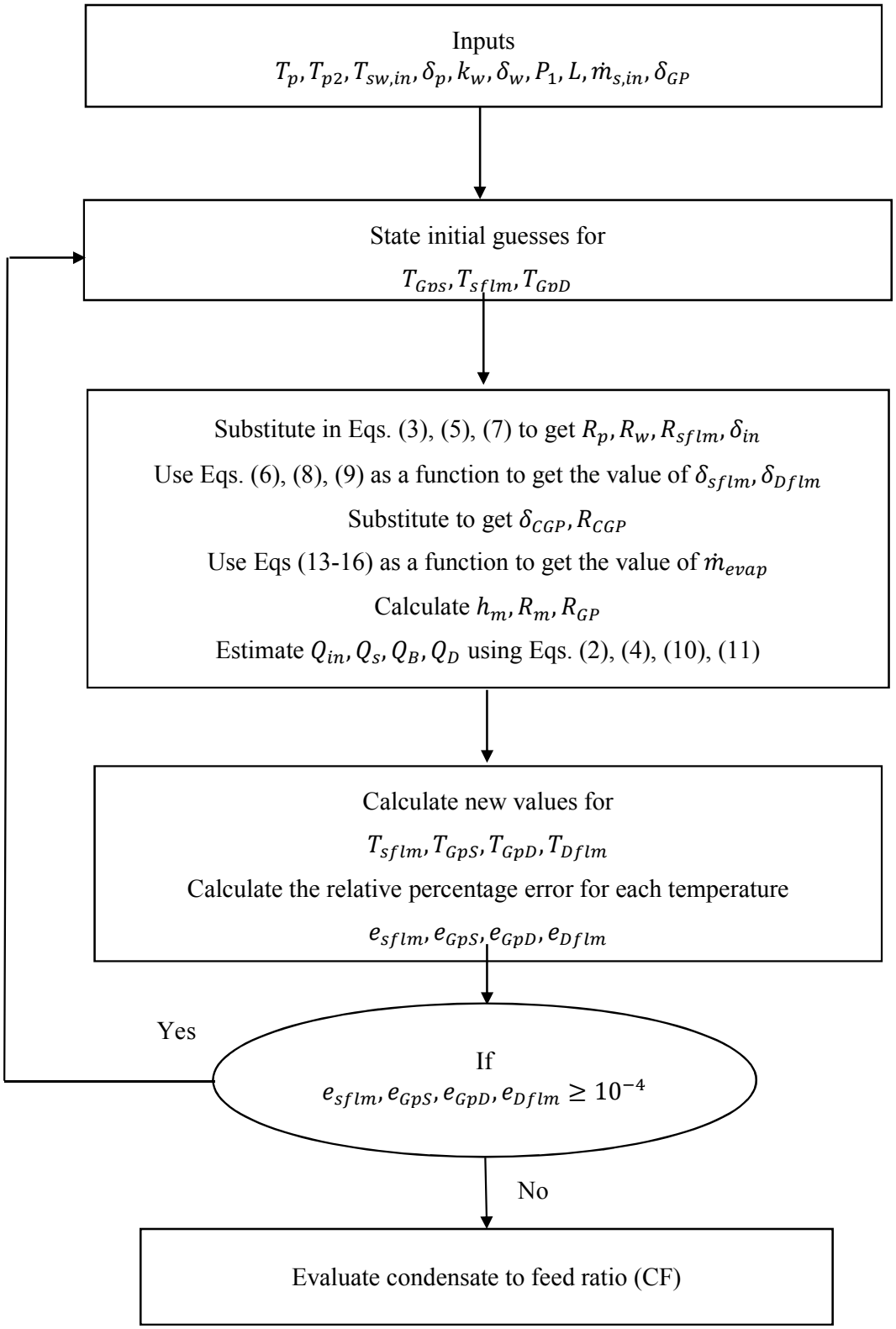

Figure 3-5: A schematic diagram of how the code works

3.2. Experimental Setup

A test rig has been built up to investigate the still's yield and to study the design parameters that may influence the productivity of the still. The experimental work aims to assess the performance and evaluate the productivity of the still for both flat and folded sheets. The test rig was constructed in a way with a view of easing assembly for both sheets. The experimental results of flat sheets have been used for verification of the code of the semi-analytical model. Furthermore, the experimental results of flat and folded sheets have been used to make a comparative study on the performance of utilizing folded sheets in the solar diffusion stills.

3.2.2. Test Rig Construction

The designed system of test rig, as shown in Figure 3-6, consists of four subsystems: heating system, feeding system, cooling system, and collecting system.

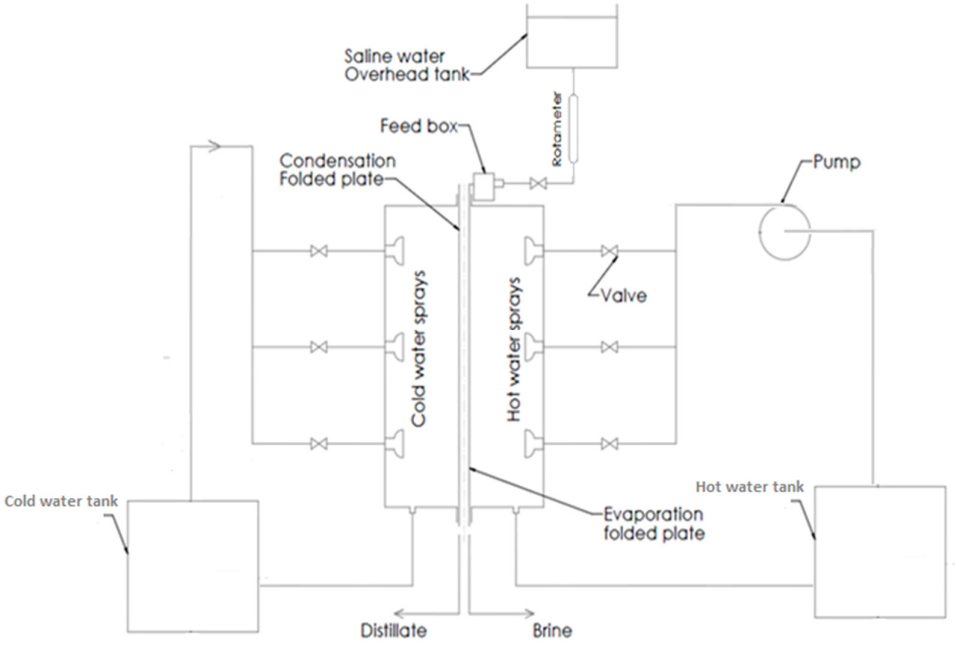

Figure 3-6: Schematic diagram for the test bench of single-effect diffusion still

First, the heating system is a closed cycle which is responsible for heating up the hot plate with the required heat to maintain its surface at constant temperature. There are three sprayers that are distributed equally on a vertical line to cover the plate and give a quite homogeneous distribution of the plate surface temperature. The sprayers are

considered as the heat source that provides the plate with continuous source of heat as follows:

The hot water is currently heated by electric heaters fixed in steel tank which is connected to a pump to lift the hot water to the sprayers then gathers in the bottom of the casing the water that keeps the sprayers to flow back to the tank throw its sump.

Second, the feeding system which is responsible for providing a steady saline film over the hot plate was a simple design that functions properly without engineering devices and mainly relies on the gravity.

Third, the cooling system provides cooling effect to the condensation plate to enhance the condensation process and makes a constant temperature distribution for the cold plate surface as a heat sink. It is similar to the heating system except it is an open loop not closed like the heating loop; the cold water is delivered from the top, and discharged by gravity.

Fourth, the collecting system which is responsible for gathering the evaporated water from the feeding saline water and at the same time collecting the condensate (fresh water); it is simply a plastic piece formed to gather each type from a side. The whole assembled system is shown in Figure 3-7.

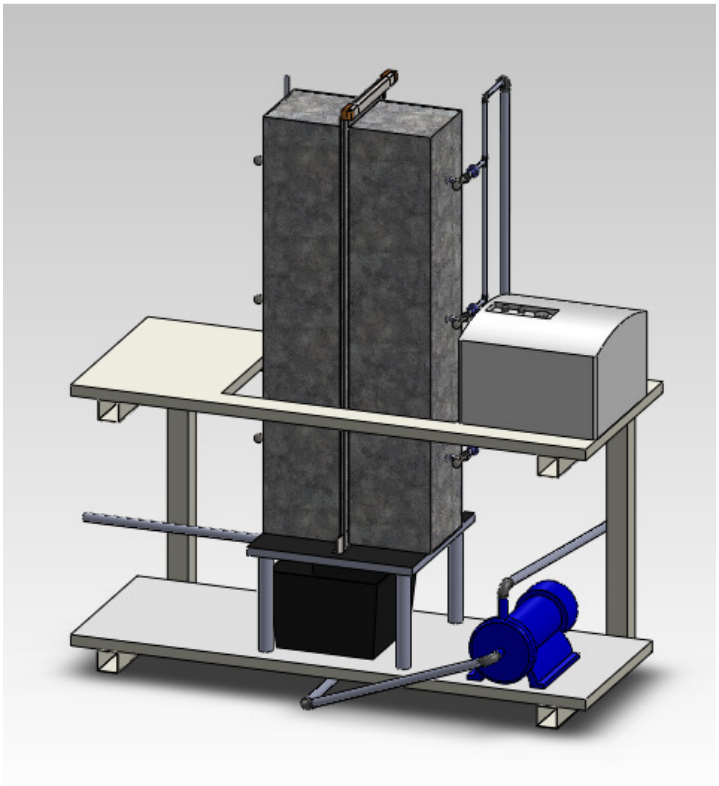

Figure 3-7: A schematic layout of the assembled test bench

In the hot loop, three sprayers have been install led to spray the water on the hot plate. The idea of using sprayers was to provide the required heat without encountering any problems with static pressure. The heating tank was meant to maintain the hot plate at constant temperature. An infrared camera has been used before the complete assembly to take a photo that shows the temperature distribution on the aluminum sheet to find out the thermal distribution. The hot plate is thermos-graphed by utilizing by infrared camera; the photos are illustrated below; before and after operating the heating cycle as shown in Figure 3-8

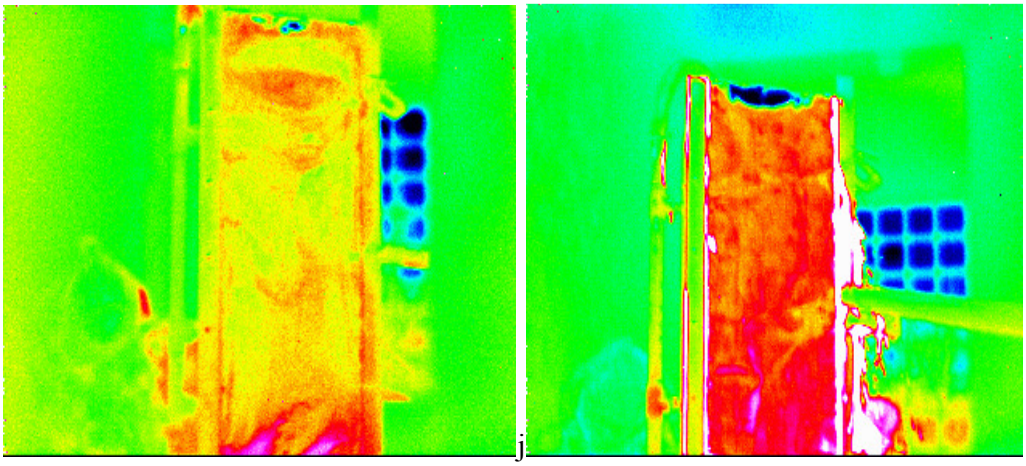

(a) Before the pump operation (b) After the operation

Figure 3-8: The thermal distribution along the sheet

Regarding the feeding mechanism, many attempts have been made to distribute the water film uniformly on its surface. The results of the trials indicated that the uniform distribution cannot be obtained without wick. The role of the wick is important due to the lack of water distribution which causes large dry patches and significant waste of input energy which, in turn, affects the validity of the experiment. In addition, the wick reduces the possibility of the contamination between the saline film and the condensate surface. Thus, a very thin piece of wick that is made of cotton has been used to guarantee a uniform and complete distribution of saline film on the hot plate. The feeding mechanism that has been installed in the system is like a rectangular box that produce a thin film over the hot plate, it is assembled over two springs that make the box flexible to adjust the film level to have a consistent flow over the plate.

.

The assembly of test bench has been designed to be able to employ both the flat and folded sheets. The experimental work has been carried out based on three stages: First, employing the flat sheet without wick. Second, employing the folded chevron-pattern sheets using wick to guarantee a good distribution of saline water over the sheet. Third, the folded chevron-pattern sheet without wick has been fixed along the sheet. With regard to the three stages, it can be clear to assess whether there is a rise in productivity of the folded over the flat and its percentage, and also the difference in productivity between the folded with wick and without wick to know which configuration is better to use later in the industrial scale.

The whole system is assembled to run the experimental work as shown in Figure 3-9.

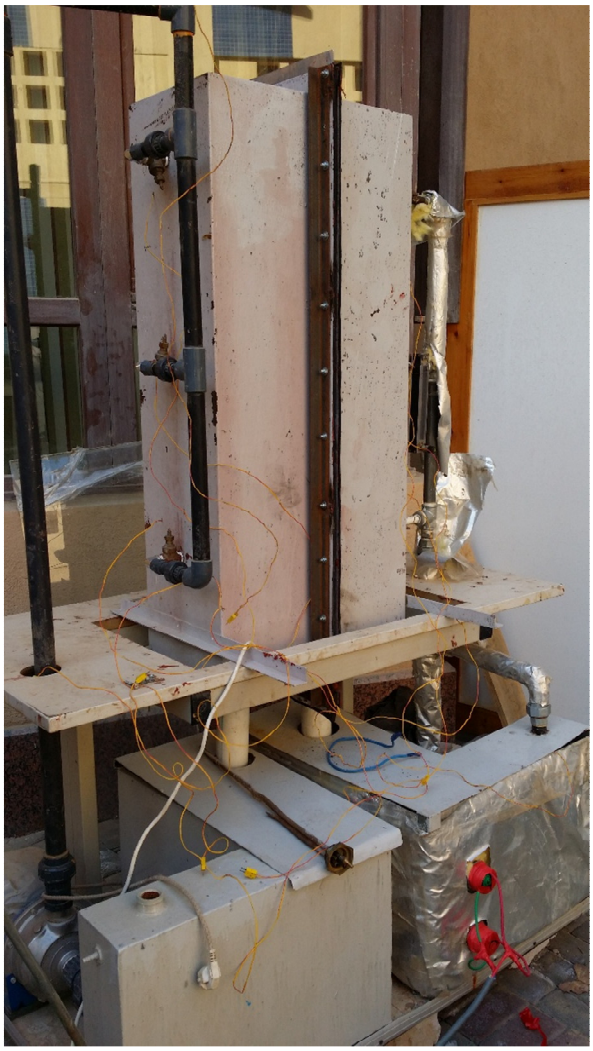

Figure 3-9: The system upon operation

3.2.3. Calibration

There are three thermocouples that have been attached to each plate over three equal spaces and its midline to make sure of the temperature of the plate. There are another two thermocouples one is inserted in the hot tank and the other in the cold tank. All the thermocouples are (K type).The calibration process of the thermocouples is performed before installing the thermocouples in the test rig. The calibration during this stage begins by placing all thermocouples in an agitated constant temperature water bath. The data logger reading is compared to a reference temperature measurement device– mercury in glass thermometer with 0.1ºC divisions. Three points are used for comparison, ice point, boiling point, and room temperature.

3.2.4. Experimental Procedure

The following steps of experimental work are chronologically presented to give an overview of how the operation process is:

1. The experiment starts by heating up the water inside the tank.
2. Then, turn on the inlet offered of saline water to fall over the hot plate, and keep the cycle warming up.
3. After the warm up period, the hot pump is turned on to pump the water from the sprayers into the hot cycle to maintain the hot plate at desired temperature.
4. Turn on the cold pump to pump the water inside the cold tank to maintain the condensate plate at the tap water temperature.
5. Fix the feed flow rate using the flow meter.
6. Let both hot and cold cycles run to reach the steady state.
7. Time out the collected brine and distilled water for a portion of time.
8. Read out the temperature of the hot water tank at the beginning of the time
9. Read out the temperature of hot water tank after the time record stop
10. Measure the collected brine and distilled.
11. Repeat the same steps from 7 to 10 as desired at different range of temperatures of the hot box
12. Change the feed flow rate via the installed flow meter and repeat the steps from 6 to 11

CHAPTER FOUR

4. RESULTS AND DISCUSSION

In this chapter the results of the semi-analytical and experimental models are discussed and presented. A parametric study is carried out to illustrate the influential parameters of the single-effect diffusion still using flat sheets. Also, a comparative study between the utilized flat and the folded sheets with wick and without wick is presented.

4.1. Flat Sheet Model

4.1.1. Model Validation

The analytical model has been developed via a software computer code using Engineering Equation Solver (EES) software to solve the equations of the semi-analytical model. It is validated against the experimental results of the test rig, and also against experimental work of El Sayed 1986 [26].Table 4-1 shows the results of the code based on the experimental results of El Sayed [26]. Then, the code results versus the experimental results and experimental results of El Sayed are plotted at Figure 4-1.

Table 4-1: The code results against the experimental results of El Sayed 1986 at (m_{in}= 0.00975 kg/m^2-s, and δ_{gap}=6 mm,$T_{s,in}$=30 °C.)

		El Sayed Experimental Results		**Code Results**	
Hot Plate Temperature T_{hp}	Cold Plate Temperature T_{cp}	Condensate	CF Experimental	CF Theoretical	Error %
°C	°C	kg/m2-h			
60	30	2.22	0.148	0.109	26.4
68	30	3.22	0.215	0.143	33.5
70	30	3.91	0.261	0.175	33.0
71	30	3.603	0.240	0.168	30.0

The conducted experimental work has been implemented inside laboratory where the temperature is 25.5 °C and relative humidity is 40%. The following Table 4-2 shows the obtained experimental results at different constant mass feed flow rates with regard to variation of hot plate temperature. In the experiment, the distillate collection process has been operated at different durations, range from (5 to 10 minutes). The readings of condensate are provided by a glass graduated cylinder of accuracy 10 ml.

Table 4-2: The experimental results of condensate-to-feed ratio variation with regard to the hot plate temperature at different mass feed flow rates with constant δ_{gap}=10 mm and T_{p2}=25.5°C.

Feed flow rate	Hot average temperature	Condensate	Feed	CF Experimental	CF Theoretical	Error
[ml/min] (Kg/m2-s)	°C	ml/min	ml/min			%
[150]	62.15	90	2000	0.047	0.04686	0.30
(0.006944)	67.35	100	1900	0.061	0.06074	0.43
	73.35	110	1600	0.080	0.08022	-0.27
	79.5	120	1600	0.105	0.1048	0.19
[267]	63.55	60	1700	0.028	0.02764	1.29
(0.01236)	69.1	90	1800	0.030	0.03016	-0.53
	73.5	100	1800	0.043	0.04311	-0.26
	77.3	110	1600	0.050	0.05043	-0.86
	80.75	125	1800	0.058	0.05787	0.22
[327]	76.5	90	1800	0.039	0.03894	0.15
(0.0151)	83.6	90	1500	0.051	0.05116	-0.31
	85.75	115	1600	0.055	0.05539	-0.71
[456]	62.2	50	2200	0.015	0.01483	1.13
(0.0211)	64.2	55	2000	0.016	0.01619	-1.19
	66.8	60	2100	0.018	0.01808	-0.44
	69.15	70	2200	0.020	0.01991	0.45
	69.8	75	1900	0.020	0.02044	-2.20

Figure 4-1compares the model results and the experimental results as well as the experimental results of El Sayed 1986 [26]. As shown in the plot the difference between the model results and experimental results may be contained in a window of error by +/-35 %. At low mass feed rates, the model results are close to the experimental results. At high mass feed flow rates, the model results over predicts the experimental results.

This may be explained as the code considers the conduction mode of heat transfer as the dominant mode which appears at the low feed flow rates which have small film thickness. As the flow rate increases the film thickness increases too and the convection component effect cannot be neglected in the process of the heat transfer through the saline film thickness. In other words, it means the assumption of Nusselts theory will collapse.

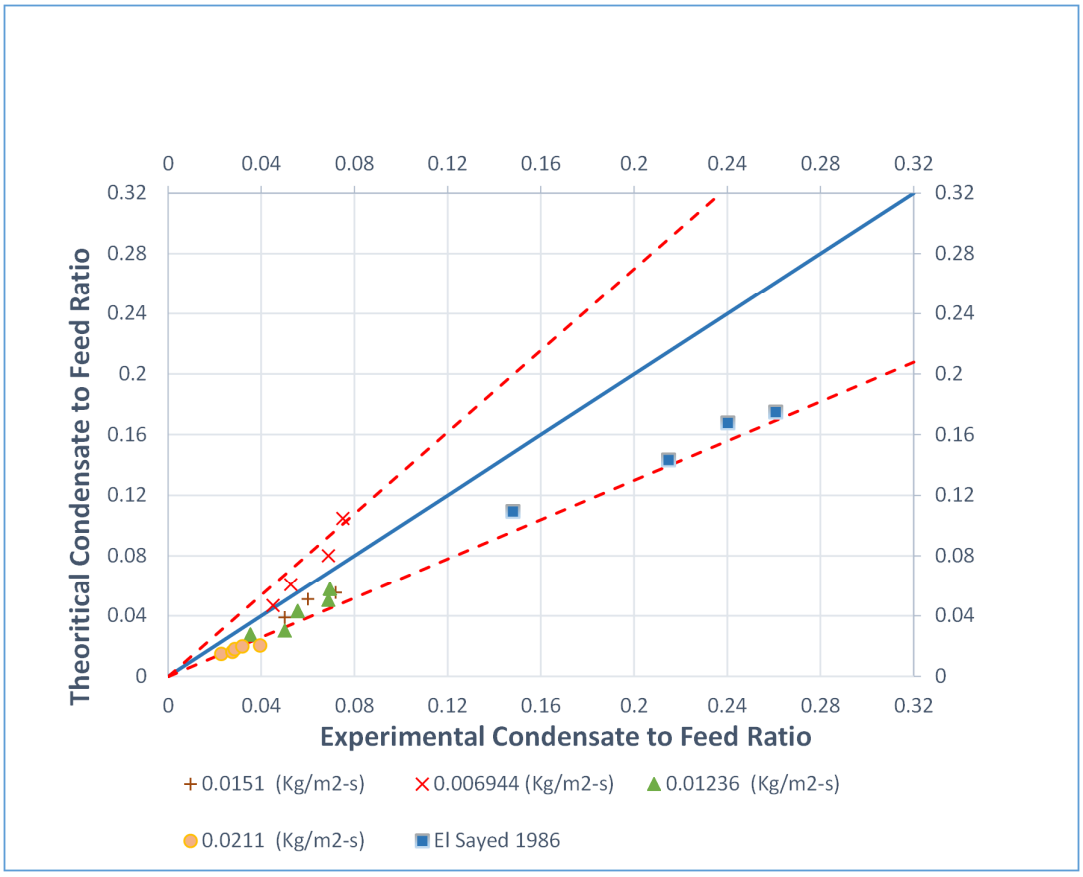

Figure 4-1: The calculated CF against the experimental CF of the experimental work and experimental work of El Sayed 1986 [26].

4.1.2. Parametric study of single-effect diffusion still using flat sheets

The semi-analytical model helps construct a parametric study to find out the dominant parameters that influence the performance of the still.

After the validation of the code against former author and the experimental results, it is important to investigate the influence of the parameters of the diffusion still. There is a need to study the substantive parameters that may dominate the performance of the still; such as the hot plate temperature, cold plate temperature, the feed water temperature, mass feed rate and diffusion gap.

The operation conditions and properties for the semi-analytical and experimental models are:

T_{amb}=28 °C	δ_{gap}= 0.1 m
T_P= 60-90 °C	$\delta_{stainlessplate}$= 0.005 m
T_{P2} =25-30 °C	$\delta_{wick} = 0.0005\ m$
T_{Sw_in}= 40 °C	h_{fg}= 2283*103 J/kg
Mw= 18	$T_m = \frac{T_p + T_{p2}}{2}$
A= 0.3 *1.2 = 0.36 m^2	P_t= 10^5 Pa
Length: 1.2 m	

The following plots present explicitly the relation between the experimental parameters against the still performance. In the experimental work, the change of the saline feed flow rate and the hot plate temperature have been considered, while the distance between the two isothermal plate, the cold plate temperature, and the inlet feed temperature are kept constant.

Figure 4-2 shows the effect of the hot plate temperature and the cold plate temperature on the condensate to feed ratio. It is clear that increasing the hot plate temperature, and decreasing the cold plate temperature increases the condensate to feed ratio. The increase of hot plate temperature leads to the increase of evaporation of the saline feed water which increases, the condensate to feed ratio. The cold plate works as a cold sink to the heat, whenever cold plate temperature decreases down, it helps enhancing the condensation of water on the cold plate, which accordingly increases the condensate to feed ratio. The hot plate temperature is exponentially proportional to the condensate to feed ratio

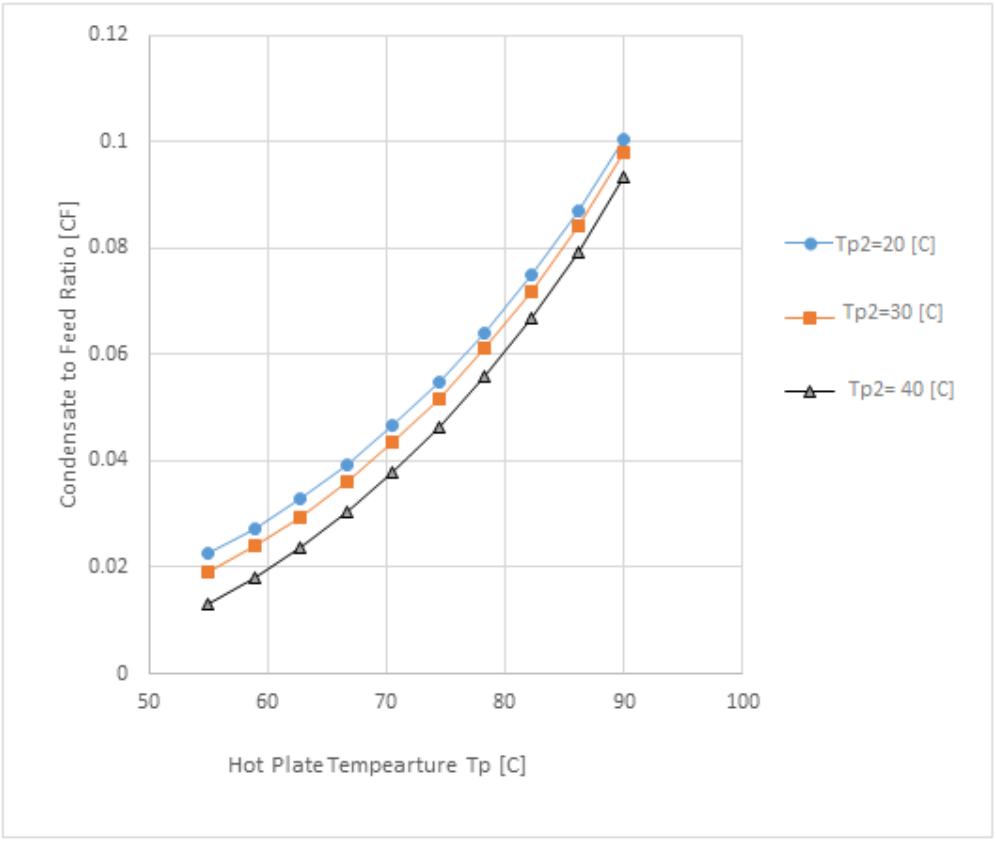

Figure 4-2: The relation between hot plate temperature T_P and the CF with different cold plate temperatures at (T_{sw_in}= 20 °C,m_{sw_in}= 0.0151 kg/m^2-S, δ_{gap} = 10 mm)

Figure 4-3 shows the effect of diffusion gap and hot plate temperature on the condensate to feed ratio. The increase of hot plate temperature or the decrease of the diffusion gap increases the condensate to feed ratio. Narrowing the diffusion gap between hot and cold plates helps enhancing the heat transfer because of decreasing the thermal resistance. The diffusion gap thickness controls the evaporation rate of the still. A lower gap thickness will increase the evaporation rate. Thus, it will be favorable in terms of productivity to reduce the gap thickness as much as possible. However, the decrease in diffusion gap thickness is quite limited to avoid the mixture between the saline feed flow and the condensate flow. The practically possible least obtained diffusion gap thickness is4 mm which is applicable for limited range of feed flow rates.

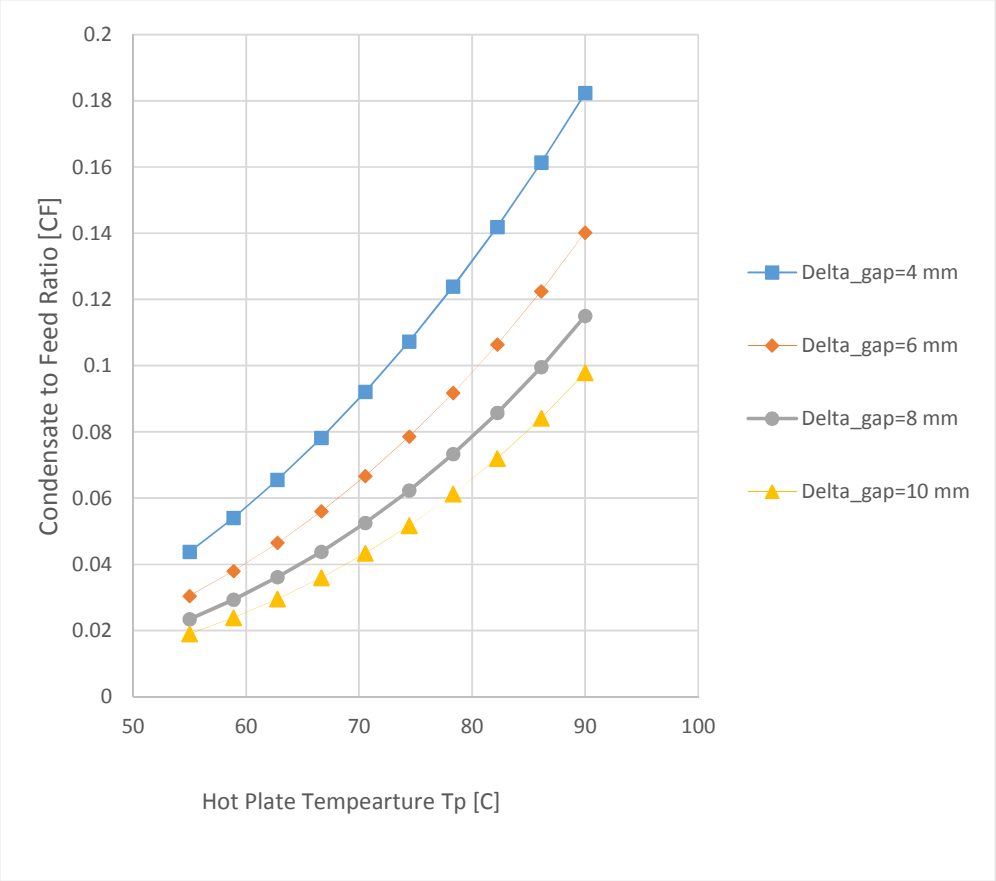

Figure 4-3: The relation between the hot plate temperature T_P and the CF with different diffusion gaps at (T_{P2} = 30 °C, T_{sw_in}= 20 °C, m_{sw_in} = 0.0151 kg/m^2-S)

Figure 4-4 shows the effect of saline water inlet temperature or the mass feed rate temperature on the condensate to feed ratio. The graph indicates that either the decrease of mass feed rate or the increase of saline water inlet temperature leads to the increase of the condensate to feed ratio. The mass feed flow rate affects the heat losses. For a fixed evaporation rate, a high saline feed rate will decrease the residence time of the saline and thus increase the amount of unutilized thermal energy exiting with it. Low saline flow rates will reduce the amount of mass and heat available for evaporation. A high saline feed rate absorbs more input heat due to a higher heat transfer coefficient. However, the productivity is decreased since the evaporation rate is saturated and the extra heat is lost with the saline film exiting the system.

In the experiment, the saline feed water has been preheated to investigate its effect on the productivity. .It is found, as shown in Figure 4-4that increasing the saline water

temperature leads to an increase in the condensate to feed ratio. But the increase is noticed to be very slight compared to the other engaged parameters.

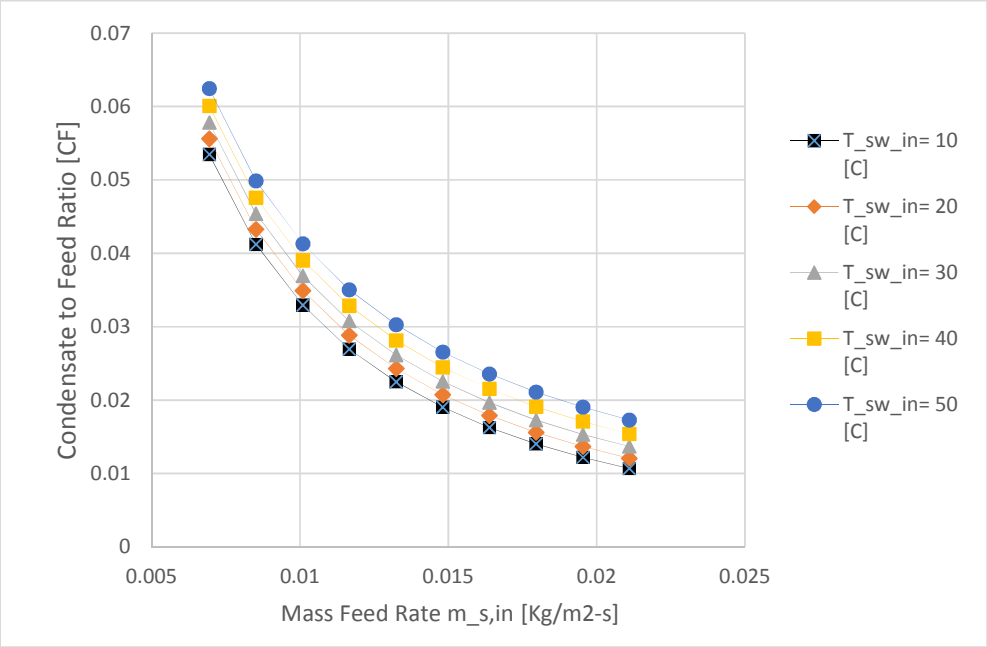

Figure 4-4: The relation between the mass feed water rate and the CF with different saline feed water temperatures at (T_P= 80 °C, T_{P2}= 30 °C, δ_{gap} = 10 mm)

The parametric study reveals the relation of the influential parameters on the still's productivity, and how they affect each other. It can be concluded that the most dominant parameters are the mass feed rate and the hot plate temperature; the plots show the relation between hot plate temperature is exponentially proportional to the condensate to feed ratio. While, the mass feed rate is inversely proportional to the condensate to feed ratio.

4.2. Folded Sheet Model

4.2.1. Model Validation

Some modifications have been adjusted to investigate the folded sheets model, the chevron type. The main change was mainly the effective length. Table 4-3 presents the model results against the experimental work.

Table 4-3: The code results against the experimental work with respect to the hot plate temperature, at (m_{sw_in} =0.00311kg/s and T_{P2} =25.5°Cand δ_{gap} = 10 mm.

Hot Plate Temperature (°C)	Experimental CF Ratio	Theoretical CF	Error %
68.73	0.083832	0.09226	9.14
70.76	0.078481	0.09683	18.95
70.93	0.079019	0.09878	20.01
70.95	0.085339	0.1021	16.42
71.20	0.07947	0.09814	19.02
71.77	0.093985	0.1046	10.15
72.17	0.081794	0.1032	20.74

Figure 4-3 shows the model results against the experimental results on folded sheet. The difference between the model results and the experimental work have been contained within a window of error of 25 %. The model under predicts the results of experimental work. This may be explained as that the model is one dimensional that works based on a uniform saline film. In the case of folded sheets, the saline film is no longer uniform, and may develop turbulence [29]. The developed code assumes the flow of the saline film to be laminar. However the chevron shape may induce turbulence, and create disturbance along the folded sheets. Thus, the code cannot predict efficiently the productivity of the still in the case of folded sheets.

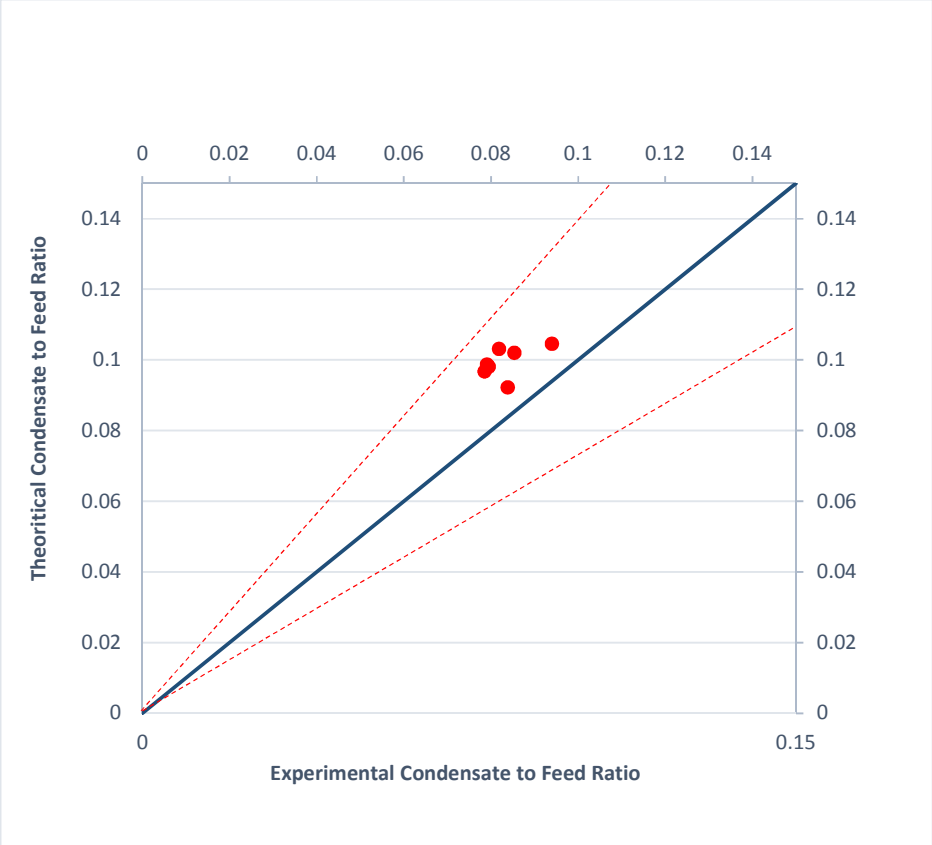

Figure 4-5: Validation curve of the folded analytical model

4.2.2. Experimental Work

The same test bench that has been utilized in flat sheet has been also used for the folded sheets. The flat sheet is replaced by the folded chevron sheet. The test bench has been operated to study the effect of hot plate temperature and saline feed flow rate on the performance ratio which is the ratio between the condensate to the feed. The experiments have been run in indoor conditions of 25.5 ^{o}C.

4.2.2.1. Folded sheets without wick

In this case, the folded sheet is installed without the wick over its surface to examine the performance of the sheet alone and assess how the folding of the chevron shape performs. As the experiments have been carried out using the flat sheet with wick to help in the equal distribution of saline over the hot plate, the need for testing folded sheets without wick has been needed to stand on better configuration of still productivity that uses folded without wick over the flat sheets. Table 4-4 shows the experimental results of condensate to feed ratio versus the hot plate temperature. The experimental results are plotted in comparison with the experimental results of flat sheet in Figure 4-6. The plot indicates that the performance of the folded sheet of chevron without wicks higher than the flat sheet.

Table 4-4: The experimental results of folded type without wick. at $m_{sw\_in} = 3.115$ ml/s

Hot Plate Temperature (°C)	Brine flow rate (ml/s)	Condensate flow rate (ml/s)	CF Ratio Experimental
68.73	1.834532	0.167866	0.083832
70.76	1.803766	0.153617	0.078481
70.93	1.849015	0.158643	0.079019
70.95	1.955098	0.182413	0.085339
71.20	1.782051	0.153846	0.07947
71.77	1.934189	0.200642	0.093985
72.17	2.013889	0.179398	0.081794

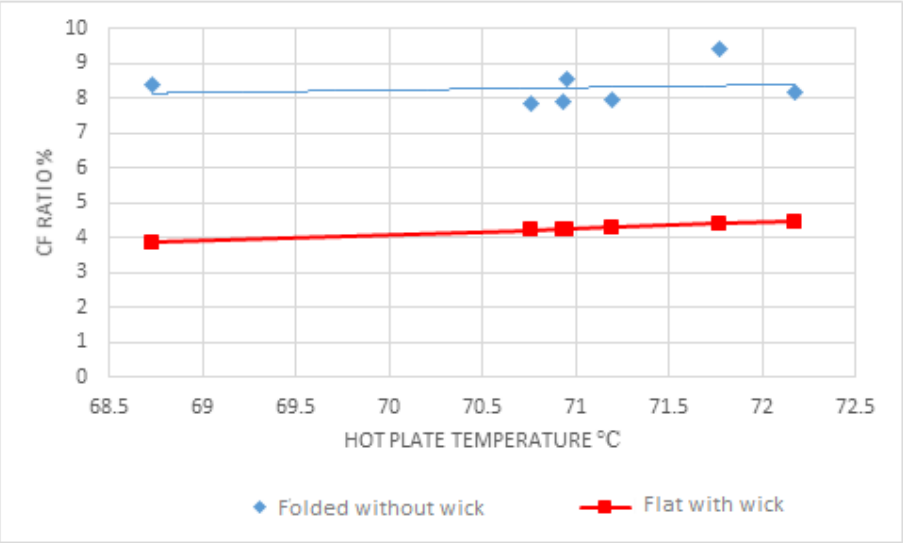

Figure 4-6:A comparison between the productivity of the flat sheets and the folded sheets without wick at m_{sw_in} = 3.115 ml/s and δ_{gap} =10 mm and T_{p2}=25 °C

4.2.2.2. Folded sheets with wick

In this case, the folded sheet replaced the flat sheet with a wick that covered the folded sheet as the same utilized with the flat sheet. Experiments have been operated using the folded Aluminum sheet using wick to help in slowing down the water feed rate and make sure of water distribution along the sheet. The temperature of the cold plate is kept constant at an average temperature of 25 °C. The air gap thickness is kept constant as well at 10 mm to get a comparable data with the data obtained from flat plate experiments. The following Table presents the experimental results of folded sheets in terms of condensate to feed ration with respect to the mass feed rate and the hot plate temperature. From Figure 4-7 to Figure 4-10, a comparative plots have been performed to compare the performance of experimental results of folded sheets to the flat sheet. The plots shows the better performance of folded sheets over the flat sheets in terms of condensate to feed ratio, with respect to the hot plate temperature and with various mass feed rates.

Table 4-5: The experimental results of folded sheet with wick with regard to hot plate temperature at various feed flow rates but constant air gap of 10 mm and cold plate temperature of 25.5 °C

Feed rate of flow [ml/s] (Kg/m^2-S)	Hot Plate Temperature (°C)	CF Ratio Experimental
[3.1155] (0.0069)	65.85	0.099441
	73	0.102597
	78.4	0.115215
	83.5	0.111806
[5.1925] (0.0124)	62	0.113257
	68.6	0.128091
	72.65	0.126156
	77.75	0.125591
	81.05	0.15265
	83.5	0.124824
[6.231] (0.0151)	62	0.088
	67	0.088
	72	0.097
	77	0.116
	81	0.131
[8.308] (0.0211)	62	0.062962
	67	0.085714
	72	0.083818
	77	0.093175
	81	0.094235

The figures 4-7 to 4-10 indicate that the productivity of the still utilizing folded sheets decreases with the increase of the feed flow rate, which is similar to what happened with the flat sheet. It is productivity of still increases with the increase of hot plate temperature for both clear that the types flat and folded that employ the wick

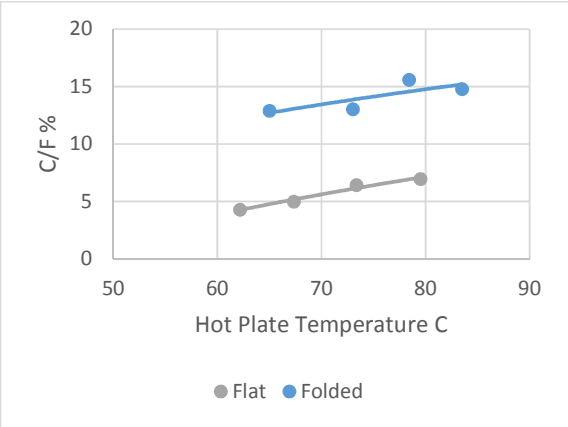

Figure 4-7: A comparison between the productivity of the flat sheets and the folded sheets with wick at m_{sw_in} = 3.115 ml/s

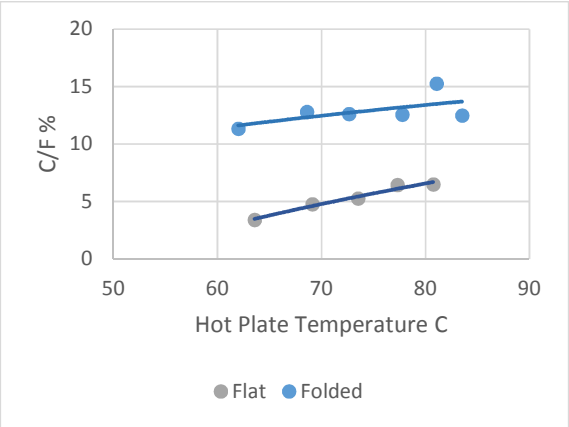

Figure 4-8: A comparison between the productivity of the flat sheets and the folded sheets with wick at m_{sw_in} = 5.1925 ml/s

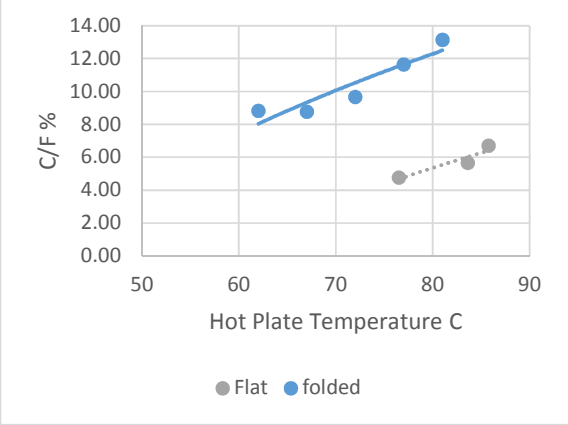

Figure 4-9: A comparison between the productivity of the flat sheets and the folded sheets with wick at m_{sw_in} = 6.231ml/s

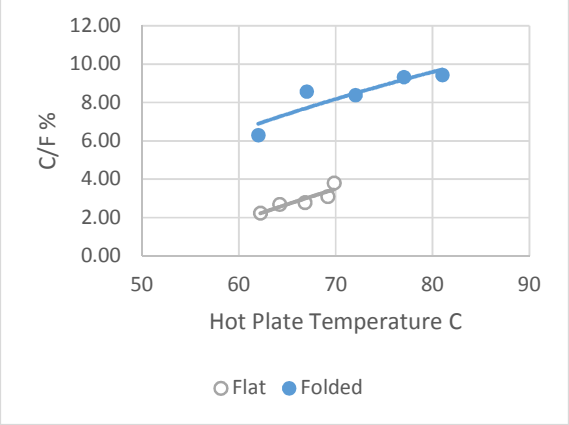

Figure 4-10: A comparison between the productivity of the flat sheets and the folded sheets with wick at m_{sw_in} = 8.308 ml/s

4.3. Comparative Analysis

The results of experimental work of the flat sheets and folded sheets both with and without wick are compared to each other. The performance of the still differs from each other with respect to the heat and mass transfer that occur between the gap of hot and cold plates. As shown below in Figure 4-11, the performance of folded with wick has a higher productivity among other sheets. It indicates the superiority of the wicked folded over the wickless folded and the flat sheet.

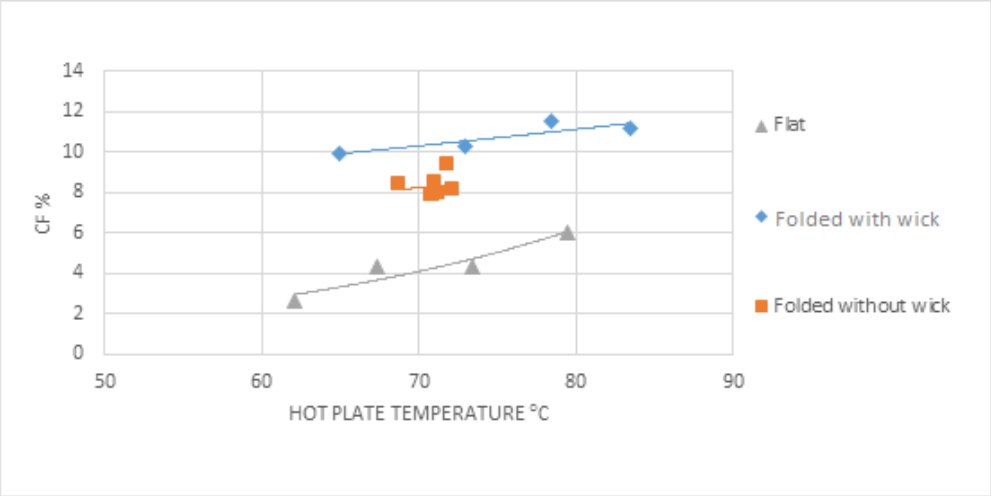

Figure 4-11: A comparison between the productivity of the flat based vertical diffusion still, folded based with wick, and the folded based without wick at feed flow rate of 3.115 ml/s and constant air gap thickness of 10 mm and constant cold plate temperature of 25 °C.

CHAPTER FIVE

5. CONCLUSION AND RECOMMENDATIONS

5.1. Conclusion

This work contributes to have better understanding of the vertical diffusion solar stills. A semi-analytical model has been developed utilizing flat sheets and folded sheets. Further, an experimental work has been carried out for the model validation. The experimental work is also installed to investigate the performance of the flat sheets and folded sheets. As a result, the semi-analytical and experimental model for the flat sheet and folded sheets have shown a good agreement. The folded sheets showed a better performance for the diffusion still with wick and without wick rather than the flat sheet. Moreover, a parametric study has been conducted on the flat sheet and showed the parameters that affect the productivity of the still.

It is found that five parameters influence the productivity of the still: the hot plate temperature, mass feed rate, diffusion gap, cold plate temperature, saline water temperature. Two of parameters have the major impact on the performance of the still; the hot plate temperature as well as the mass feed rate. The productivity increases when the hot plate temperature increases and the mass feed rate decreases.

A comparative study has been presented and compared the performance of wickless and wick folded sheets and the flat ones. The folded chevron-pattern sheets using wick that have been experimentally investigated showed rise in performance better around the flat sheets by 27 % . It can be concluded that the folded sheets utilization has a better productivity.

5.2. Recommendations for Future Work

This study of single-effect diffusion solar still utilizing folded sheets was a step, and still further research is required yet to become effectively applicable and economically feasible. The area of solar stills is broad, and the application of folded sheets is also new. Thus, here are some highlights for further research:

- Integrate solar heaters with the diffusion still instead of the utilized electric heaters.
- Develop a semi-analytical model for the multiple-effect-diffusion solar still for flat sheets.
- Investigate the performance of the still using different materials of folded sheets like stainless steel, and copper.
- Develop a semi-analytical model for the multiple-effect diffusion still utilizing folded sheets.
- Make a parametric study about the multiple-effect diffusion still utilizing folded sheets.
- Investigate the performance of different patterns of the folded sheets.
- Make an economical study and cost-benefit-analysis for the multiple-effect diffusion solar still

REFERENCES

[1] World Business Council for Sustainable Development, Facts and Trends: Water, WBCSD, 2009. [Online]. Available: www.wbcsd.org/Pages/EDocument/EDocumentDetails.aspx?ID=137. [Accessed September 2013].

[2] United Nations world water development report, Executive Summary, Water for People, Water for Life, Paris, France, UNESCO publishing, 2003. [Online]. Available: webworld.unesco.org/water/wwap/wwdr/wwdr1/. [Accessed September 2013].

[3] U.S. Bureau of reclamation and Sandia National Laboratory, Desalination and Water Purification Technology Roadmap, National Technical Information Service, "A Report of the Executive Committee spring field," 2003. [Online]. Available: www.usbr.gov/research/AWT/s_t_publications/Desal%20Roadmap.pdf. [Accessed September 2013].

[4] United Nations Population Division, [Online]. Available: www.un.org/esa/population/publications/sixbillion/sixbilpart1.pdf. [Accessed July 2014].

[5] Sampathkumar, K., Arjunan, T.V., Pitchandi, P., and Senthilkumar, P., "Active solar distillation—A detailed review," *Renewable and Sustainable Energy Reviews,* vol. 14, p. 1503–1526 , 2010.

[6] K. S. Tree, "Water Industry Report on Desalination," World Trade Center San Diego, 2013.

[7] Kaushal, A., and Varun, "Solar stills: A review," *Renewable and Sustainable Energy Reviews,* vol. 14, no. 1, pp. 446-453, 2010.

[8] Rajaseenivasan, T., Murugavel, K.K., Elango T.,and Hansen, R.S., "A Review of Different Methods to Enhance the Productivity of the Multi-Effect Solar Stil," *Renewable and Sustainable Energy Reviews,* vol. 17, p. 248–259, 2013.

[9] Tanaka, H., Nosoko, T., and Nagata, T., "A highly Productive Basin-Type-Multiple-Effect Coupled Solar Still," *Desalination,* vol. 130, pp. 279-293, 2000.

[10] Tanaka, H., Nosoko, T., and Nagata, T., "Experimental Study of Basin-Type, Multiple-Effect, Diffusion-Coupled Solar Still," *Desalination,* vol. 150, no. 2, pp. 131-144, 2002.

[11] Tanaka, H., Nakatake, Y., "A Vertical Multiple-Effect Diffusion-Type Solar Still Coupled With a Heat-Pipe Solar Collector," *Desalination,* vol. 160, pp. 195-205, 2004.

[12] Tanaka, H., "Experimental Study of Vertical Multiple-Effect Diffusion Solar Still Coupled with a Flat Plate Reflector," *Desalination,* vol. 249, no. 1, pp. 34-40, 2009.

[13] Basily, B. B., Elsayed, A. E. and Daniel, K., "Technology for Continuous Folding of Sheet Materials". Patent 7,115,089, 3 October 2006.

[14] Basily, B. B., Elsayed, A. E. and Daniel, K., "Technology for Continuous Folding of Sheet Materials". Patent 7,691,045, 6 April 2010.

[15] R. Dunkle, "Solar Water Distillation: The Roof Type Still and a Multiple-Effect Diffusion Still," *International Heat Transfer Conference, University of Colorado,* vol. 5, pp. 895-902, 1961.

[16] Cooper, P.I., Appleyard, J.A., "The construction and performance of a three effect, wick-type, tilted solar still," vol. 12, pp. 4-8, 1967.

[17] K. Selcuk, "Design and Performance Evaluation of A Multiple-Effect, Tilted Solar Distillation Unit," vol. 1, no. 8, 1964.

[18] Elsayed, M., Fathalah, K., Shams, J., and Sabbagh, J., "Performance of Multiple Effect Diffusion Stills," *Desalination,* vol. 51, pp. 183-199, 1984.

[19] M. M. Elsayed, "Effects of Parametric Conditions on the Performance of an Ideal Diffusion Still," *Applied Energy,* no. 22, pp. 187-203, 1986.

[20] Garter, F., Durrbeck, M., Rheinlander J., "Multi-effect Still fot Hybrid Solar/Forssil Desalination of Sea and Brackish Water," *Desalination,* vol. 138, pp. 111-119, 2001.

[21] Tanaka, H., NakatakeY., Watanabe, K., "Parametric Study on a Veritcal Mutiple-effect diffusion-Type Solar Still Coupled with a Heat-Pipe Solar Collector," *Desalination,* vol. 171, pp. 243-253, 2004.

[22] Tanaka, H., Nakatake, Y., and Tanaka, M.,, "Indoor Experiments of the Vertical Multiple-Effect Diffusion-Type Solar Still Coupled with a Heat-Pipe Solar Collector," *Desalination,* vol. 177, no. 1-3, pp. 291-302, 2005.

[23] Bouchekima, B., Gros, B., Ouaches, R., and Diboun, M., "The Performance of The Capillary Film Solar Still Installed in South Algeria," *Desalination,* no. 137, pp. 31-38, 2001.

[24] E. V. Somers, "Theoretical Considerations of Combined Thermal and Mass Transfer from a Flat Plate," *ASME J. Appl. Mech,* vol. 23, p. 295–301, 1956.

[25] T. Nosoko, T. Kinjo, C.D. Park, "Theoretical analysis of a multiple-effect diffusion still producing highly concentrated seawater," *El SEVIER, Desalination* , vol. 180, pp. 33-45, 2005.

[26] Fathalah, K., Elsayed, M., Taha, I., and J. Sabbagh, "Numerical Study of Evaporation –Condensation in a Vertical Diffusion Gap," *Warm-und Stoffubertragung,* vol. 20, pp. 301-309, 1986.

[27] Tafreshi, V., Ercan, E., Poirdeyhimi, B., "Calculating Mass Transfer From Vertical Wet Fabrics Using a Free Convective Heat Transfer Correlation," vol. 42, pp. 767-769, 2006.

[28] Churchill, S.W., and Chu, H.H., "Correlating Equations for Laminar and Turbulent Free Convection From A Vertical Plate.," *Int. J. Heat Mass Transfer,* vol. 18, pp. 1323-1329, 1975.

[29] Raach, H., and Mitrovic, J., "Seawater Falling Film Evaporation on Vertical Plates with Turbulence Wires," *Desalination,* no. 183, p. 307–316, 2005.

[30] Raach, H., and Mitrovic, J., "Simulation of Heat and Mass Transfer in a Multi-Effect Distillation Plant for Seawater Desalination," *Desalination,* Vols. 1-3, no. 204, pp. 416-422, 2007.

[31] Incropera, F., Dewitt, D., Berman, T., Lavine, A., Fundamentals of Heat and Mass Transfer, Sixth ed., Wiley, pp. 643-648.

[32] ISO (1980): International Organization of Standards. ISO 1438/1-1980(E). Water flow measurement in open channels using weirs and venturi flumes, Part 1: Thin plate weirs.

[33] Elsayed, E. A. and Basily, B. B., "A Continuous Folding Process for Sheet Material," *International Journal of Materials and Product Technology,* vol. 21, pp. 217-238., 2004.

[34] Cheng, L.I., and Junming, L.I., "Laminar Forced Convection Heat and Mass Transfer of Humid Air Across a Vertical Plate With Condensation," *Chinese Journal of Chemical Engineering,* vol. 19, no. 6, pp. 944-954, 2011.

[35] Desrayaud, G., and Lauriat, G., "Heat and Mass transfer analogy for Condensation of Humid air in a vertical Channel," *Heat and mass transfer, Springer,* no. 37, pp. 67-76, 2001.